2011

Evaluation of simultaneous water and gas injection using CO2

Shrinidhi Shetty
Louisiana State University and Agricultural and Mechanical College, sshett1@tigers.lsu.edu

EVALUATION OF SIMULTANEOUS WATER AND GAS INJECTION USING CO_2

A Thesis
Submitted to the Graduate Faculty of the
Louisiana State University and
Agricultural and Mechanical College
in partial fulfillment of the
requirement for the degree of
Master of Science in Petroleum Engineering

In

The Craft & Hawkins Department of Petroleum Engineering

by
Shrinidhi Shetty
B.E. Visvesvaraya Technological University, India, 2005
May 2011

Dedicated

To My Beloved Parents Sadashiva Shetty P and Suphala Shetty

My Advisor Dr. Richard Hughes

and

My Friends

ACKNOWLEDGEMENTS

I would like to thank Louisiana State University for providing the environment to pursue my graduate study. I would like express my sincere gratitude and appreciation to my adviser Dr. Richard Hughes for his guidance, encouragement and support throughout my graduate study

I would also like to thank Dr. Dandina Rao and Dr. Seung Ihl Kam for accepting to serve on my exam committee and helping in enhancing this work. A special thanks to all the faculty and staff members of Craft and Hawkins Department of Petroleum Engineering for their contribution towards my education. A special thanks to Darryl Bourgoyne for his technical guidance; without him setting up the laboratory would have been even more difficult. Also, I would like to thank Fenelon Nunes for "all time help" in purchasing and safe operation of the laboratory. Thanks to Dayanand Saini, Paulina Mwangi, Gbola Afonja and Venugopal Rao Nagineni for the technical input and support during this work.

A special appreciation and thanks to Abhijeeth Rai, Darshan Shetty, Guruprasad Shetty, Laxmish Pandith, Leela Madhav Gullapalli, Pratheek Shetty, Ravi Sondur, Sanjay Patil, Satheesh K.A, Shefali Shetty, Shruti Shetty, Sunaina Jain, Sushanth Shetty, Swathi Shetty and Swatin Shetty for the unrelenting love, encouragement and support especially during not so good times. You guys are valuable to me.

I would also like to thank Harsha Chatra, Vinay Raghuram, Pratap Bhat, Ajay Kardak, Ajay Ravichandran, Tejaswini Narayana, Poornima Narayanan, Rahul Gajbhiye, and Sneha Panchadhara for making my stay at Baton Rouge a memorable one. You guys have always been wonderful.

I would also like to thank my aunt and uncle Dr. Hema Ballal and Raj Ballal, for their love and affection. A special thanks to my uncle and aunt Dr. Anand Shetty and Suchi Shetty for

being my guardians in the U.S. Lastly and most importantly thanks to two of the most wonderful people in my life; my parents, Sadashiva Shetty P and Suphala Shetty for being my support system.

Support for this work was provided in part by the U.S. Department of Energy under Award Number DE-FC-26-04NT15536. Neither the United States Government nor any agency thereof, nor any of their employees, makes any warranty, express or implied, or assumes any legal liability or responsibility for the accuracy, completeness, or usefulness of any information, apparatus, product, or process disclosed, or represents that its use would not infringe privately owned rights. Reference herein to any specific commercial product, process or service by trade name, trademark, manufacturer, or otherwise does not necessarily constitute or imply its endorsement, recommendation, or favoring by the United States Government or any agency thereof. The views and opinions of authors expressed herein do not necessarily state or reflect those of the United States Government or any agency thereof.

TABLE OF CONTENTS

LIST OF TABLES

LIST OF FIGURES

NOMENCLATURE

A	Cross sectional area of the core
B	Formation volume factor
G	Gas Volumes
K	Permeability
L	Length
M	molecular weight
N	oil volume
N_{ca}	capillary number
Q	Volumetric flow rate
R	Gas solubility
S	Saturation
u	Superficial velocity
dp/dx	Pressure gradient
f	Fractional flow.

Subscripts

i	initial
o	oil
w	water
g	gas
wc	connate water

wi	initial water
oi	initial oil
or	residual oil
ro	relative to oil
rw	relative to water
p	produced
sc	at standard conditions of pressure and temperature.
wf	water flood
TF	tertiary flood

Superscripts

*	limiting value
o	end point

Abbreviations

BP	Back pressure
CGI	Continuous Gas Injection
DAQ	Data Acquisition
IFT	Interfacial tension
IPA	Isopropyl alcohol
MMP	Minimum Miscibility Pressure
OOIP	Original Oil in Place

PV	Pore Volumes
PVI	Pore Volumes Injected
ROIP	Residual Oil in Place
SWAG	Simultaneous Water and Gas Injection.
TRF	Tertiary Recovery Factor
UF	Gas Utilization Factor
VIT	Vanishing Interfacial tension
WAG	Water Alternating Gas

Greek

μ	Dynamic viscosity
ɵ	Contact angle
σ	Interfacial tension
ϕ	Porosity
ρ	Density

ABSTRACT

Miscible CO_2 injection is the second largest contributor to global enhanced oil recovery, as it has successfully undergone extensive laboratory tests and field applications for recovering residual oil left behind after waterflooding. Prolific incremental recoveries have been obtained for some fields. Although miscible CO_2 injections generally have excellent microscopic displacement efficiency they often result in poor sweep efficiency. In order to address sweep problems and maximize recoveries, other schemes of gas injection have been developed. Two such processes are water-alternating-gas (WAG) and simultaneous water-and-gas (SWAG) injection. WAG and SWAG have been successfully used to minimize poor sweep. Improved gas utilization and oil recovery have been reported for SWAG injection at Joffre Viking, Kapurak River, and Rangley Weber fields.

There are very little published data evaluating the performance of simultaneous water and gas injection under miscible conditions and very little published data exists that compares enhanced recovery processes conducted under consistent experimental conditions. This is especially true when the gas is CO_2. In this work a sequence of experiments were conducted to evaluate core flood behavior of Continuous Gas Injection (CGI), 1:1 Water Alternating Gas (WAG) with a slug size of 0.25 pore volumes, and Simultaneous Water-and-Gas (SWAG) injection at four f_g values. The experiments were conducted at rock wettability, flow rates and pressures that were as consistent as possible in order to make meaningful comparisons. After 2 PV of CO_2 injection the SWAG flood with f_g = 0.4 recovered about 0.9692 of waterflood residual oil. CGI had the second best recovery of about 0.8998 followed by WAG with 0.8602. The SWAG flood with f_g = 0.6 recovered about 0.8300 of waterflood residual oil and SWAG with f_g = 0.8 and f_g = 0.2 recovered about 0.7507 and 0.7253 respectively. The gas utilization

was the least for SWAG with f_g = 0.4 at 15.54 Mscf/bbl followed by CGI with 16.13 Mscf/bbl. The remaining experiments utilized over 17.20 Mscf/bbl.

1 PROBLEM STATEMENT

Gas injection is the largest contributor to oil recovered by any enhanced oil recovery process. Oil production from gas injection reported by Moritis (2010) was about 371 Mbbl/day. Of the 130 active gas injection projects, 109 utilized miscible CO_2 enhanced recovery schemes and accounted for 272 Mbbl/day second only to thermal recovery at 292 Mbbl/day (Moritis, 2010).

Continuous injection of CO_2 as an enhanced oil recovery process is very well understood from micromodel and coreflood experiments. The displacement efficiency is high under miscible conditions and lower when not. However, at the field-scale fluid mobility, gravity, reservoir heterogeneity, and viscosity all result in poor sweep efficiency resulting in large amounts of residual oil. Water alternating gas (WAG) injection is the most common mobility control technique employed by the industry, while foams (Chang and Grigg, 1994; Espinoza et al., 2010) and viscosifiers (Enick et al. 2000; Heller et al., 1985) are being investigated and slowly being implemented.

Simultaneous water and gas injection (SWAG) is a process that has been also developed for conformance control and has been less rigorously studied. A few of the laboratory scale studies have reported better sweep while field scale implementations of the process have inferred better sweep from higher recoveries. A detailed description of a number of the studies is available in Appendix A. These studies will be reviewed briefly in order to provide the motivation for work in this thesis.

Caudle and Dyes (1958) reported higher sweep efficiency of about 90 percent from miscible SWAG compared to about 60 percent from injection of miscible gas. Tiffin and Yellig (1983) stated that the total recoveries from SWAG injection were functions of total injection rate and the fractional flow values of the gas. Sohrabi et al. (2008) observed no dependence of oil

recoveries on gas fractional flow values. Chang and Grigg (1999) reported two flow regime behavior during simultaneous water and CO_2 injection with a critical value of gas fractional flow (f_g^*) of 0.333 indicating dispersion of CO_2 in water. Sohrabi et al. (2008) did not observe any bubbles and the liquid and gas flow paths were separate. Bortkevich et al. (2006) developed equipment to create a micro-dispersed gas-liquid mixture that had stable bubble sizes much smaller than the typical pore throat diameters. Further the micro-dispersed gas-liquid mixture injection with gas content of 10-40 percent recovered additional of about 153993 barrels of residual oil from 90 wells in the Samotlor field in West Siberia (Bortkevich et al., 2005).

A simultaneous water-and-CO_2 injection pilot was implemented at Joffre Viking field at a gas to water ratio of 1 (corresponding to an f_g value of 0.5) and resulted in improved recovery as compared to water alternating CO_2 injection and continuous CO_2 injection (Stephenson et al., 1993). Simulation and design optimization studies of water-alternating-gas (WAG) injection at the Rangley-Weber field reported that average fractional flow of oil would increase by 10 % over 1:1 and 2:1 WAG with a slug size of 0.3 PV. Further, smaller WAG half cycles would result in higher CO_2 retention due to reduction in fingering (Attanucci et al., 1993). The fluctuations in gas-liquid ratio value were considerably reduced along with a positive change in the decline rate of oil production previously observed under WAG (Robie et al., 1995). A fully compositional simulation study of simultaneous water and CO_2 injection at the Kapurak River field showed that SWAG with CO_2 would enable better conformance control and reduce gas handling costs compared to WAG (Ma et al., 1995). Subsequent field tests of SWAG with static mixtures resulted in a dispersed flow based on reasonable agreement between measured and no slip pressure drop calculations of bottom hole pressures (Stoisits et al. 1995). The SWAG injection was carried out in the Siri field using the produced gas (Berge et al., 2002; Quale et al., 2000). The ability of the SWAG process in effective implementation of mobility control has

been reported consistently as discussed earlier. However, some of the contradictory observations reported for the SWAG process needs to be addressed by obtaining more consistent experimental data allowing meaningful comparisons between the CGI, SWAG and WAG processes.

1.1 Summary and Motivation

As previously discussed, CGI and WAG processes have been extensively studied (Green and Willhite, 1998; Lake, 1989). However, comprehensive studies on the SWAG process are less available even though sweep improvement with SWAG has been reported. Caudle and Dyes (1958) and Sohrabi et al. (2008) have reported sweep improvement by SWAG based on micromodel studies. In addition Sohrabi et al. (2008) also reported that oil recoveries are independent of fractional flow of gas value of SWAG, while Tiffin and Yellig (1983) observed dependence of SWAG recoveries on fractional flow of gas, total injection rate and rock wettability. Stoisits et al. (1995) reported bubbly flow of CO_2 and water by using static mixers. Chang and Grigg (1999) used a filter during simultaneous injection of CO_2 and water observed the two flow regime. Sohrabi et al. (2008) without a static mixer observed separate flow of methane and water. Bortkevitch et al. (2005) patented an apparatus for producing micro dispersed gas liquid mixture with bubble size 0.3 times the average pore throat diameter for better reservoir sweep. The micro-dispersed gas-liquid mixture process recovered additional 153993 barrels of residual oil in the Samotlor field which was inferred to be due to enhanced sweep. The motivation behind the work presented in this thesis is to test whether SWAG process using CO_2 depends on the expensive patented apparatus and to critically evaluate the mechanism behind any success the process has on improving recoveries. This work will also evaluate whether similar behavior to published work can be obtained with CO_2 as the solvent. In addition the work intends to answer the ambiguity about dependence of oil recovery on fractional flow value of gas and to test possible dispersion of CO_2 in water.

2 EXPERIMETAL DESCRIPTION

In order to achieve the objectives of the study as described in section 1.1, it was necessary to perform a series of experiments under the conditions that are as consistent as possible. The following six experiments were performed:

- Experiment #1: Continuous Gas Injection (f_g) = 1.
- Experiment # 2: SWAG at fractional flow of gas (f_g) = 0.2.
- Experiment #3: SWAG at fractional flow of gas (f_g) = 0.4.
- Experiment #4: SWAG at fractional flow of gas (f_g) = 0.6
- Experiment #5: SWAG at fractional flow of gas (f_g) = 0.8
- Experiment #6: WAG (1:1) with slug size of 0.25 pore volume.

All the experiments were performed until 2 pore volumes of CO_2 had been injected.

2.1 Factors Influencing Flood Performance

In order to make meaningful comparisons between the above mentioned experiments, it was necessary to maintain experimental conditions that are close to being consistent. Some of the important factors affecting the consistency of experimental conditions are rock wettability, minimum miscibility pressure, brine composition and injection rates. In order to minimize the variation in each of these factors, experiments were performed using the same core and similar conditions with suitable fluids that maintained conditions as close to consistent as possible.

2.1.1 Wettability

Craig (1971) defined wettability as “the tendency of one fluid to spread on or adhere to a solid surface in the presence of other immiscible fluids”. In a rock-oil-brine system, wettability is an indicator of rock preference to either oil or water. Wettability is a major factor controlling the distribution and flow of fluids in a given porous medium. In general, cleaned sandstone cores are

strongly water-wet as cleaning solvents should flush any adsorbed foreign material. The composition of crude oil and the salinity and pH of the brine are important in determining the wettability (Anderson, 1986).

One way to infer wettability of a system is through the connate water saturation and end point relative permeability values. Craig (1971) provided rules of thumb as shown in Table 1 (Craig, 1971). Wettability alteration can be inferred from changes in the characteristics of the relative permeability curves (Rao et al., 2006).

Table 1: Craig's Rules of Thumb (Craig, 1971)

Wettability Criterion	Water-Wet Rock	Oil Wet Rock
S_{wc}	>20- 25%	<15%
k_{ro}°	>80-95%	70%
k_{rw}°	<30%	>50%

2.1.2 Minimum Miscibility Pressure (MMP)

Minimum miscibility pressure (MMP) is the lowest pressure at which the interfacial tension between a pair of fluids vanishes. Some of the commonly used experimental techniques to understand gas-oil miscibility are; phase behavior measurements, slim-tube tests, the rising bubble technique and the vanishing interfacial-tension (VIT) technique.

Reamer and Sage (1963) performed phase behavior measurements on a CO_2/n-decane system at a variety of temperatures to obtain the pressure-composition two phase envelope. At a temperature of 38 ^{o}C and pressures greater than 1150 psi, the CO_2 and decane were single phase fluids (Reamer and Sage, 1963). Glass (1985) defined MMP for a slimtube test as: “the lowest pressure at which, we have a distinct point of maximum curvature when recovery of oil is plotted

against pressure at 1.2 PV gas injected". When the point of maximum curvature is not clearly evident, the 95% recovery of oil at 1.2 PV can be used as a benchmark to define MMP (Glass, 1985).

Elsharkawy et al. (1992) compared the MMP values of a CO_2/n-decane system obtained using slimtube tests with measurements using the rising bubble technique both at 38 ^oC. An MMP of 1200 psi was reported using the benchmark of 95% recovery, while it was reported to be 1280 psi using the rising bubble technique. The rising bubble technique was quicker and more reliable than the slim tube tests and does not really have a standard procedure to determine MMP (Elsharkawy et al., 1992). The MMP values obtained from the rising bubble technique closely matched those from slim-tube tests.

Rao (1997) developed a new technique called the vanishing interfacial tension (VIT) for miscibility determination. The IFT measured between the oil and gas at first contact is a measure of first-contact miscibility and IFT measurement after attaining equilibrium represents multi-contact miscibility (Rao, 1997). Ayirala and Rao (2006) reported an MMP of 1160 psi for the CO_2/n-decane system using the VIT technique at 38 ^oC. The phase behavior study to quantify the MMP of two fluids is expensive, cumbersome and time consuming. The VIT technique was the cheapest, quickest and consumed least quantity of fluids compared to slim-tube and phase behavior experiments. It is qualitative and more accurate than rising bubble measurements which are based on visual observations (Ayirala and Rao, 2006).

Kulkarni (2003) performed miscible CO_2 floods with a back pressure value of 2500 psi with n-decane. In the work presented here, the core floods were performed with a back pressure of 2400 psi to ensure miscibility.

2.1.3 Berea Sandstone

The rock used in all experiments was a cylindrical core of Berea sandstone shown in Figure 1. The core was one inch in diameter and one foot long.

Figure 1: Berea Sandstone Core

Berea sandstone is mainly comprised of quartz, with traces of feldspar and kaolinite. However analysis of fines less than 2 μm reported the presence of 79 percent of kaolinite (Shaw et al., 1991) as shown in Table 2. Azari and Leimkuhler (1990) and Gabriel and Inamdar (1983) reported similar results.

Table 2: Composition of Berea Sandstone (Shaw et al, 1991)

Mineral %	Bulk Analysis	Fine Analysis(<2μm)
Quartz	82.5	2.0
Feldspar	3.8	0.8
Calcite	trace	-
Dolomite	1.2	trace
Kaolinite	9.7	79
Chlorite	1.3	3.5
Illite/Mica	1.5	7.3
Siderite	-	-
Illite/Smectite	-	7.4
Total Clay	12.5	

2.1.4 Experimental Fluids

To minimize the effects of significant changes in wettability on flooding performance, neutral oil like n-decane should be used. The exposure of the core to n-decane has little effect on

the native wettability of the core demonstrated by approximately consistent values of connate water saturations and end-point phase permeabilities with divalent brines (Kulkarni, 2003).

In order to have a consistent pore structure throughout the experiment, it was necessary to have stable clays. One of the major reasons for permeability reduction in Berea sandstone was identified as release of clay particles into the flowing fluid eventually blocking the pore throats that are smaller than the particles. The release of these particles is strongly dependent on the concentration, type and valence of the ions in the water. When divalent ions are present in the brine, they are adsorbed by the surface of clay particles with full surface coating eliminating formation damage (Gabriel and Inamdar, 1983; Kia et al., 1987; Kulkarni and Rao, 2004). Some crude oil recoveries are sensitive to brine salinity while mineral oils are independent of salinity (Sharma and Filoco, 2000). Hence 2% by weight calcium chloride was used to prepare the brine to minimize the release of clay particles and subsequent effects on flooding performance. The properties of the fluids used in the experiments presented in this thesis are shown in Table 3.

Table 3: Experimental Fluid Properties

Fluid	**Density 2500 psi, 24^o C (gm/cc)**	**Viscosity 2500 psi, 24^o C (gm/cc)**	**Density 14.7 psi, 24^o C (gm/cc)**
2% $CaCl_2$ Brine (McCain Jr., 1990)	1.0124	1.1	1.0090
n-Decane (NIST, 2008b)	0.7388	1.0256	0.7273
CO_2 (NIST, 2008a)	0.8948	0.0901	0.0018

SUDAN-4 dye was used to color the decane to distinguish the water from the oil. The chemicals used for cleaning the core, dye and $CaCl_2$ salt were supplied by Fisher Scientific, New Jersey. The brine was prepared using de-ionized water. All the experiments were performed on Berea sandstone with a back pressure of 2400 psi. The oil was n-decane while the water was 2

weight percent of calcium chloride brine. The tertiary recovery fluid was dense CO_2. The experimental condition provides "dense" CO_2 because room temperature (24 ^oC) was less than critical temperature (30.9 ^oC) and the dense CO_2 properties are similar to supercritical ones. The chemicals used for core cleaning were methylene chloride, toluene and isopropyl alcohol or methanol. The experimental apparatus will be discussed in section 2.2.

2.2 Experimental Apparatus

The schematic of the core flood apparatus is as shown in Figure 2. The setup consists of (a) a core holder, (b) injection system, (c) production system, and (d) data acquisition system. A picture of the laboratory were this study was performed is shown in Figure 3.

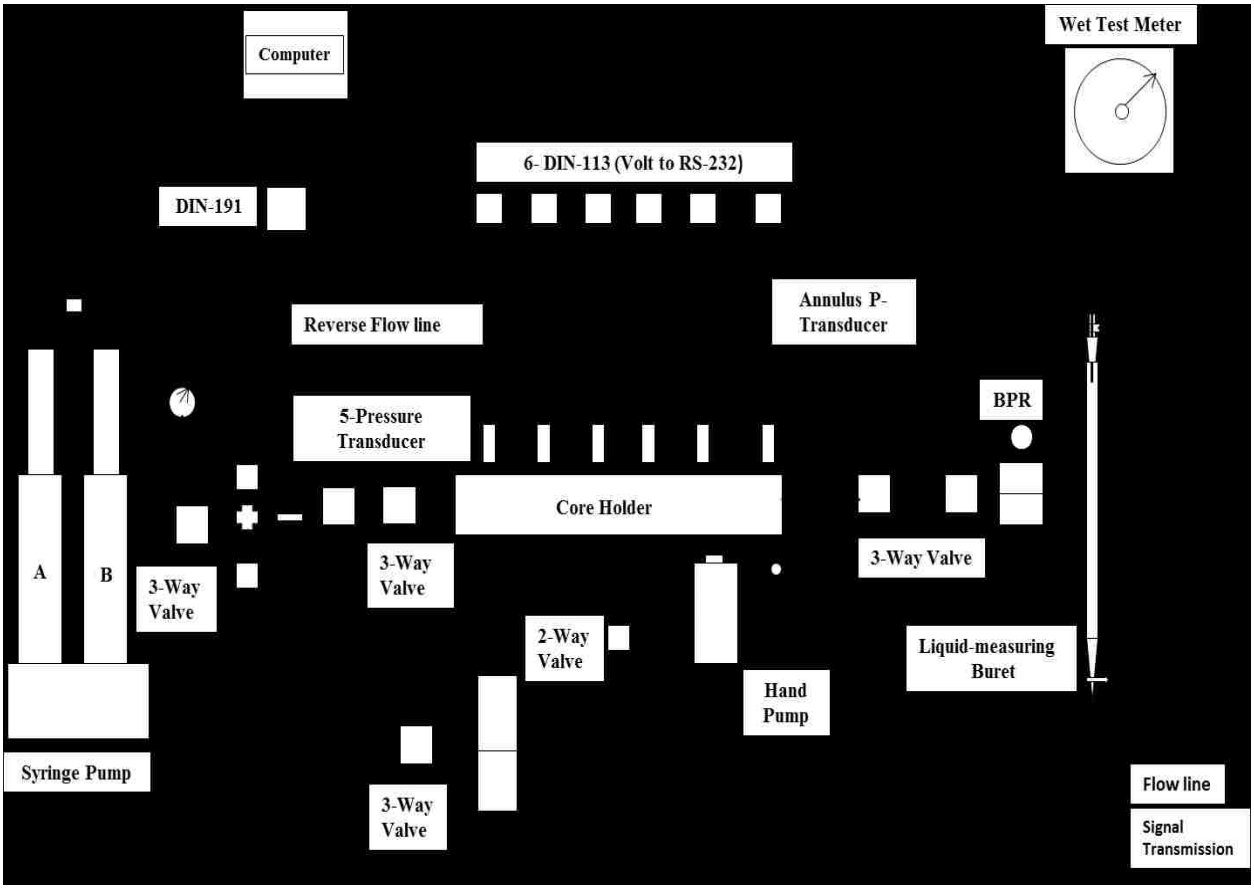

Figure 2: Schematic of High Pressure Core Flood Apparatus

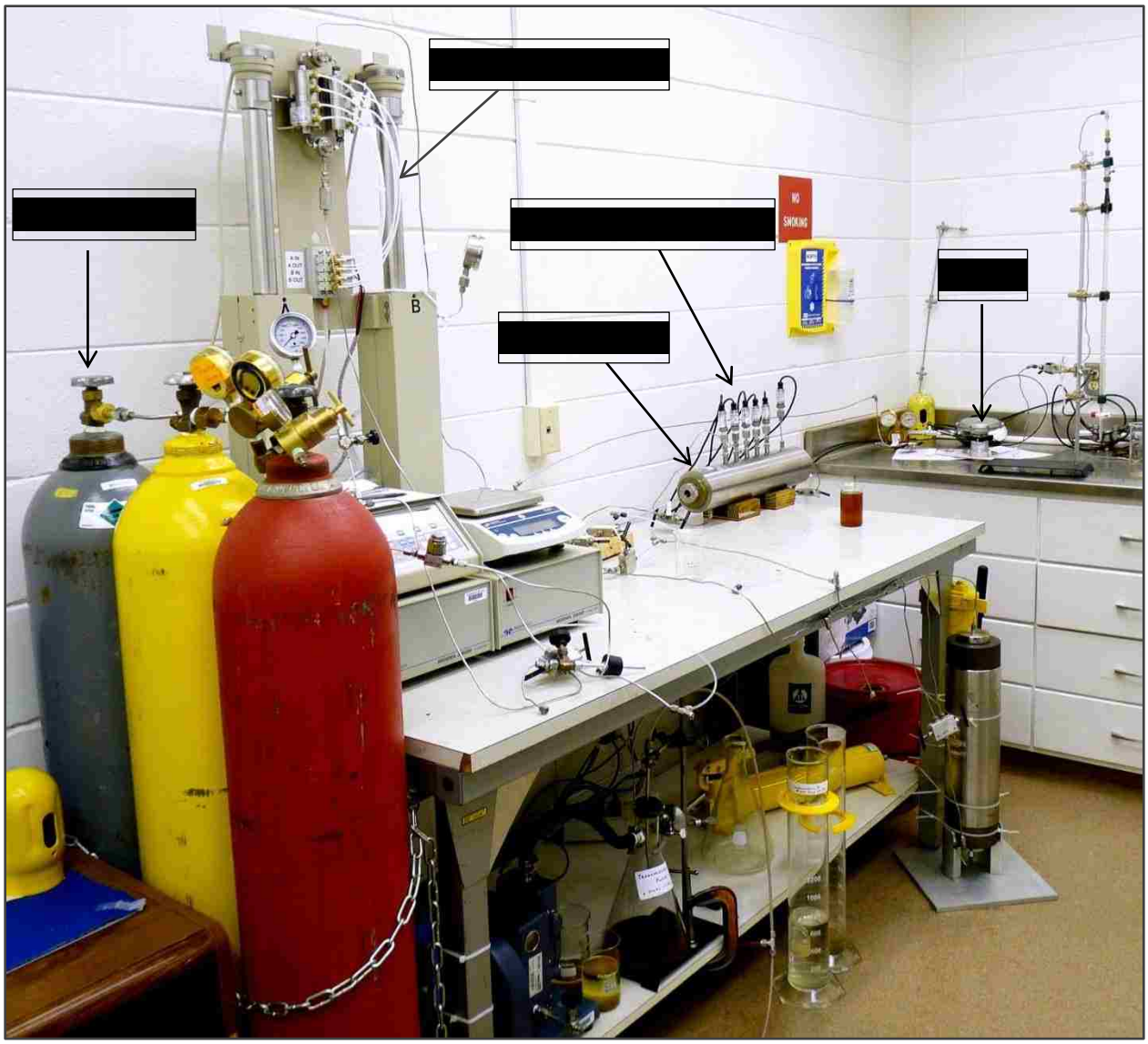

Figure 3: Hughes Group Core-Flood Laboratory

2.2.1 Core Holder

The core holder employed during this study was a Hassler-type core holder with five pressure ports and a pressure rating of 5000 psi. It was designed to house cylindrical cores of 1 inch diameter and 12 inch length. The core was enclosed in a Viton® sleeve within the stainless steel casing. The volume between the casing and the sleeve was used to apply an annulus pressure of 3000 psi, using hydraulic oil and a hand pump. End caps and the Viton® sleeve ensure isolation of the reservoir fluid from the hydraulic oil. The five pressure ports span the length of the core and are spaced at equal distance from each other. The first five pressure ports

(moving from inlet to outlet) were for measuring pressure in the core, and the sixth port was for monitoring the annulus pressure.

2.2.2 Injection System

The main components of the injection system were two ISCO syringe pumps, a 2 micron filter, a transfer vessel and various valves and tubing.

The two syringe pumps are coupled by a continuous flow valve package and have a pressure rating of 7500 psi. The combination of tubing, joints and valves form the high pressure (5000 psi max) flow conduit. The filter was used to mix the two fluids (brine and CO_2) during the tertiary SWAG floods along with screening of particles for single phase displacements. A transfer vessel equipped with a piston was employed only during the core cleaning procedure in order to isolate the pump from cleaning fluids. The cleaning fluids were injected into the core by pumping distilled water into the bottom of the transfer vessel with the cleaning fluid in the top of the vessel.

2.2.3 Production System

A back pressure regulator, a graduated burette and a wet test meter along with the valves, joints and tubing formed the production system.

The back pressure regulator was a dome-type air-loaded actuator set to maintain a constant system pressure (rated to 2500 psi with an accuracy of 1%). It was connected at the outlet of the core holder to maintain a system pressure of 2400 psi, to ensure miscibility between oil and CO_2 during tertiary flooding. The outlet of the back pressure regulator was connected to a graduated burette to collect the produced fluid. The gas collected in the burette was allowed to flow through the wet test meter. Forward or reverse flow directions could be achieved by activating certain valves in the system. Reverse flow was necessary for efficient core cleaning.

2.2.4 Data Acquisition System

The components of the data acquisition module were pressure transducers, an Omega DIN-113 for each transducer, an Omega DIN-191, a 5 volt DC power supply and a Microsoft Excel® data acquisition program. The five transducers measured pressures along the length of the core and a transducer was employed to monitor the annulus pressure. The transducers acquired the pressure data as a function of time. The voltage signals from each transducer were processed and converted to RS-232 communication signals by their respective Omega DIN-113. All of the RS-232 signals were further converted to the correct electrical signal required by the RS-485 using a single Omega DIN-191. Generally RS-485 signals are recommended when many modules and devices must be connected to a host computer over a long distance. The individual RS-485 signals were acquired by a Microsoft Excel® program developed by Darryl Bourgoyne, from the Petroleum Engineering Research and Technology Transfer Laboratory (PERTL) at Louisiana State University. This code is shown the Appendix D.

2.3 Experimental Procedure

After the core flood apparatus was built, tested and calibrated, the experimental study was performed. Three types of experiments were carried out: continuous gas injection (CGI), water alternating gas (WAG) and simultaneous water and gas (SWAG) flooding. Each of the experiments underwent a consistent sequence of cycles before undergoing tertiary flood. The sequence was: core cleaning, flooding with brine to determine absolute permeability; oil flood to connate water saturation; and waterflood to residual oil saturation. After the oil flood to connate water saturation stage, the end-point relative permeability to oil was established. After the waterflood to residual oil saturation stage, the end-point permeability to water was established. In immiscible two phase flow through porous media, capillary phenomenon is a concern. The capillary pressure (the difference between wetting and non-wetting phase pressures) depends on

curvature of the interface between the two fluids, the wettability and the pore geometry (Amyx et al., 1960). Laboratory displacement processes are almost always affected by viscous instabilities and end effects. These affects are minimized using the Rapoport and Leas (1953) scaling criterion for stabilized floods. The scaling criterion used has found to minimize the dependence of oil recovery on the injection rate and length of the core.

$$L u \mu \geq 1 \quad \text{.....(2-1)}$$

where, L is the length of the core (cm), u is Darcy velocity (cm/min) and μ is the viscosity of displacing fluid (cP).

The immiscible floods in this work were designed to operate at a scaling criterion of approximately 8.9 to ensure the stability of the floods. A Rapoport and Leas scaling coefficient of greater than 1 would minimize the capillary end-effects (Rapoport and Leas, 1953).

2.3.1 Determination of the Porosity

Before installing the core in the core holder the porosity of the core was experimentally measured using the following sequence:

1. The average diameter and length of the core were measured to calculate the average bulk volume. Three diameter measurements were made along the length of the core and a mean value for the bulk volume was used for the rest of the procedure.
2. The core was then heated in an oven to a temperature of 120 ^{o}C for 3 hours to eliminate moisture. The hot core was allowed to cool in the oven and then weighed.
3. The core was placed in a simple glass evacuation chamber. The air was evacuated from the chamber using a vacuum pump. The vacuum pump was run for about 20 min. Brine (2 wt% $CaCl_2$) was then introduced into the vacuum tight container, until the core was completely submerged in the brine solution. The core was submerged for 10-15 min.

4. The core was then removed from the vacuum chamber and gently wiped to remove any water on the surface. The brine saturated core was weighed to calculate the mass of liquid in a pore volume.
5. With a known value for density of the brine solution under the laboratory conditions, the value for the pore volume was computed.
6. The porosity of the core was determined by using

$$\phi = \frac{Pore\ Volume}{Bulk\ Volume} \quad \text{..... (2-2)}$$

2.3.2 Core Cleaning

A core exposed to reservoir fluids must be cleaned and flushed of all fluids, in order to return to something close to its initial state. This was done by removing all the fluids from the core using an extensive core cleaning procedure. During this step, cleaning fluids were run with sufficient back pressure (2400 psi) and at a high rate of 3 cc/min for efficient core cleaning. The fluids used for this procedure were: 2% $CaCl_2$ brine (normal brine), methylene chloride (buffer), isopropyl alcohol or methanol (dehydrating agent), and toluene (oil phase solvent). The following core cleaning procedure was performed after every experiment:

1. The core was flooded with 4-5 pore volumes of normal brine to remove the traces of CO_2 in the core.
2. 2 PV of methylene chloride was injected as a buffer between the cleaning fluids to prevent direct contact.
3. 2 PV of toluene was flushed through the core to dissolve residual decane in the core.
4. A buffer of methylene chloride (2 PV) was flushed through the core.
5. 2 PV of isopropyl alcohol or methanol was injected which acts as a dehydrating agent to remove any traces of brine and also helps to dissolve traces of decane left behind by

toluene. Methanol was chosen instead of a stronger dehydrator like acetone due to its incompatibility with the Viton® sleeve in the core holder. Isopropyl alcohol was used as the dehydrator during the core cleaning before Experiment #1 and #2. Methanol replaced isopropyl alcohol during the remaining core cleaning procedures.

6. 4 PV methylene chloride was used in the final flush of the core. Here 2 PV of methylene chloride flowed from inlet to outlet followed by 2 PV flowing from outlet to inlet. At the end of this process a clear effluent should be and was observed as shown in the right most beaker shown in Figure 4.

Figure 4: Effluent Produced during Core Cleaning Procedure (Left to Right)

7. Methylene chloride was displaced from the core using 2 PV normal brine solution. This was followed by a 2 PV normal brine solution flowing from outlet to inlet. Since reservoir brine salinity was low, the displacement was conducted with the 2% $CaCl_2$ brine. If the brine salinity is high, a step-wise salinity increase or decrease is recommended in order to prevent salinity shock that releases the clays present in the core.

2.3.3 Measurement of Absolute Permeability

1. After the core was cleaned, the air in the core was evacuated using a Welch Duo-Seal vacuum pump.
2. Cylinder B was flushed with isopropyl alcohol and then with distilled water to clean the cylinder.

3. About one PV of brine was injected into the core at rate of 3 cc/min prior to the measurement of absolute permeability to ensure that the core was completely saturated with brine.
4. Steady state pressure drops were measured at 2 cc/min, 1.5 cc/min and 1 cc/min.
5. The absolute permeability of the core is determined using Darcy's law:

$$k = \frac{Q\mu}{A\left(\frac{dp}{dx}\right)} \quad \text{.....(2-3)}$$

where, k is the absolute permeability of the core to brine (Darcy), Q is the constant injection rate (cc/sec), μ is the absolute viscosity of the injected fluid (cP), A is the cross sectional area of the core perpendicular to the flow (cm^2) and dp/dx is the pressure drop per unit length (psi/cm).

2.3.4 Oil Flood to Connate Water Saturation

Once the absolute permeability was measured, the brine was displaced by oil. Oil was drawn into cylinder B and then pumped into the core at a predetermined rate.

1. Cylinder B was flushed with isopropyl alcohol during experiments 1 and 2 followed by n-decane. Methanol was used to flush the cylinder followed by n-decane during all other experiments.
2. The cylinder was then filled with decane and pressurized to 2500 psi before allowing it to flow through the core.
3. The pump was set at constant rate of 1.5 cc/min, to satisfy the Rapoport and Leas (1953) criterion with the back pressure valve set to 2400 psi.
4. The volumes of brine and oil produced, as well as the pressure drop values were measured as a function of time.
5. The oil flood was carried out until 3 PV of decane had passed through the core. This was deemed sufficient to establish connate water saturation.

6. The flow rate was then reduced to 1.25 cc/min. The system was allowed stabilize and the corresponding pressure drop was measured as a function of time in order to determine the end-point effective permeability to oil. Injection rates of 1 cc/min and 0.75 cc / min were also used to subsequently verify the consistency of the end-point oil permeability.
7. The connate water saturation was calculated using material balance.

2.3.5 Waterflood to Residual Oil Saturation

The core was allowed to sit for 12 hours. Brine was used to displace the oil from the core. The procedure followed was:

1. Cylinder B was flushed with isopropyl alcohol during experiments 1 and 2 followed by distilled water. Methanol was used to flush the cylinder followed by distilled water during all other experiments.
2. The pump was then filled with 2% $CaCl_2$ brine. The brine was pressurized to 2500 psi before injecting into the core.
3. The brine was injected at 1.4 cc/min to satisfy the Rapoport and Leas (1953) scaling criterion.
4. The volumes of brine and oil produced and the corresponding pressure drop values were recorded as a function of time.
5. The flood was carried until at least 2 PV of brine had been injected.
6. End point effective permeability to brine was determined at injection rates of 1.25 cc/min, 1.0 cc/min and 0.75 cc/min. Steady state pressure drops were measured at each rate to check for consistent results.
7. The residual oil saturation was calculated using material balance.

Once the residual oil saturation was attained, the system was ready for the tertiary flood process.

2.4 Tertiary Floods

2.4.1 Continuous Miscible CO_2 Flood

For the continuous CO_2 flood, the core was injected with supercritical CO_2 at a pressure above the minimum miscibility pressure between CO_2 and n-decane using pump A. The procedure followed was:

1. CO_2 was drawn into cylinder A, and pressurized to 2500 psi, before allowing it to flow through the core.
2. The pressurized CO_2 was injected at a rate of 0.333 cc/min. Note that even though Rapoport and Leas (1953) scaling criterion is applicable to immiscible floods, the values of scaling coefficient for this miscible flood was 0.176 due to the low CO_2 viscosity.
3. The volumes of brine, oil and CO_2 produced were measured as functions of time.
4. The flooding was carried out until 2 PV of CO_2 had been injected.
5. At the end of the CO_2 flood, the injection was continued at three different rates (0.25, 0.2 and 0.15 cc/min). At each rate the system was allowed to stabilize and the steady state pressure drops were measured to check the consistency of the three end-point effective permeability values.

2.4.2 Miscible-SWAG Flood

For the simultaneous water and gas injection, the following procedure was utilized.

1. Cylinder B was flushed with IPA followed by a distilled water flush only during experiment 2. In all other experiments methanol was used to clean the cylinder followed by distilled water flush.
2. CO_2 and brine solution were loaded into two separate pumps (A and B respectively) and pressurized to 2500 psi, before allowing them to flow through the core.

3. Both the CO_2 and brine were allowed to sit overnight, to prevent instabilities and early breakthrough of displacing fluid(s) during the flood.
4. The total injection rate was set at 0.5 cc/min. Different gas fractional flow values were achieved by changing both gas and water injection rates.
5. The simultaneous water and gas injection was carried out until 2 PV of CO_2 had been injected.
6. The volumes of oil, water and CO_2 produced were recorded as functions of time.

2.4.3 Miscible-WAG Flood

For the WAG flood, the following procedure was utilized:

1. Cylinder B was flushed with methanol followed by distilled water.
2. CO_2 and brine were drawn into cylinders A and B respectively.
3. Both fluids were pressurized to 2500 psi and allowed to attain similar pressures overnight.
4. Alternate 0.25 PV slugs of CO_2 and brine were injected at 0.333 cc/min.
5. The injection continued until 2 PV of CO_2 had been injected.
6. During this process, the pressure drop values and the liquid and CO_2 production rates were measured as functions of time.

In Chapter 3 we will present the results of all the experiments followed by a section on discussion of these results

3 RESULTS AND DISCUSSION

The main objectives of this study were to determine the effect of fractional flow of gas on simultaneous water and gas (SWAG) injection process in recovering residual oil in place and comparing the SWAG performance with the conventional continuous gas injection (CGI) and water alternating gas (WAG) injection processes under the conditions that are as consistent as possible. To minimize wettability issues n-decane was chosen as the hydrocarbon phase which has shown to be neutral in wettability alteration as discussed in 2.1. In order to minimize the variations in experimental conditions all the experiments were conducted with the same Berea sandstone core.

3.1 Experimental Challenges and Procedural Changes

At the end of the CGI and SWAG with f_g = 0.2 experiments, there was a 32.5% and 35.2% drop in absolute permeability respectively. This occurred even after using a divalent $CaCl_2$ brine, thought to chemically inhibits clay dispersion, that has a demonstrated ability to stabilize the dominant dispersive clays in Berea sandstone (Kia et al., 1987; Kulkarni, 2003). A literature review suggested that even in the presence of the chemically compatible brine, the absolute permeability of a core can be reduced by mechanical dispersion by exceeding the critical superficial velocity at which the clays are dispersed. At a critical velocity greater than 0.007 cm/sec for a 150 mD Berea sandstone and $CaCl_2$ brine, clays were dispersed mechanically. The degree of permeability reduction is a function of flow velocity, direction, initial permeability and wettability (Gabriel and Inamdar, 1983). The maximum brine superficial velocity used in our experiments was 0.0059 cm/sec. This suggests that the permeability reduction observed was not due either to chemical or mechanical induced dispersion of clays. With further investigations the interaction between the brine and isopropyl alcohol was identified as the likely source of permeability reduction. Salts may have precipitated when isopropyl alcohol came in contact with

the brine leading to two successive reductions in absolute permeability. Possible dehydrators to replace isopropyl alcohol were acetone, chloroform methanol azeotrope or methanol. Methanol was chosen as acetone was highly incompatible with Viton® sleeve in the core holder, while chloroform methanol azeotrope has a low flash point. Hence methanol was used as a dehydrator during the cleaning process from Experiment #3 onwards. The drop in absolute permeability was stabilized after the use of methanol as is evident from the values of absolute permeability, connate water saturation and end-point permeabilities.

3.2 Experimental Results

Each of the six experiments performed had undergone the same sequence of cycles: primary imbibition, primary drainage (oil flood), secondary imbibition (water flood) and finally tertiary flood. Each experiment is summarized in Tables 4 and 5, and will be discussed in the sections that follow.

3.2.1 Primary Drainage (Oil-Flood)

In Figures 6-8, the graphs labeled figure (a) show the normalized water recovery and pressure drops obtained from the data recorded during primary drainage of each experiment. The cumulative water recoveries were plotted as the ratio of change in water saturation to the initial water saturation ($[S_{wi}-S_w]/S_{wi}$). Oil floods in all the experiments were designed to be carried out at 1.5 cc/min with the Rapoport and Leas (1953) scaling coefficient of 8.94.

The oil with lower mobility compared to the water tries to displace the water from the pores; this causes the pressure drop across the core to build up until oil breaks through. After breakthrough, the pressure drop decreases and stabilizes to an approximately steady state at connate water saturation. The approximately steady-state pressure drop in experiments 1, 2 and 3 was about 35 psi, 50 psi and 135 psi respectively. With all other conditions being similar the increase in pressure drop was most likely due to the drop in the absolute permeability from 68.75

mD to 46.43 mD and then to 30.13 mD along with consequent variations in end point relative permeability to oil.

Table 4: Summary of Oil and Water Floods

Exp. #	*Description*	*BP (psi)*	*k (mD)*	S_{wc}	k_{ro}°	$(S_{or})_{wf}$	k_{rw}°	*WaterFlood Recovery (OOIP)*
1	CGI	2400	68.75	0.4895	0.6220	0.3600	0.0833	0.2945
2	SWAG $f_g = 0.2$	2400	46.43	0.4209	0.6338	0.3911	0.1066	0.3245
3	SWAG $f_g = 0.4$	2400	30.13	0.4410	0.5865	0.3479	0.0986	0.3775
4	SWAG $f_g = 0.6$	2400	29.15	0.4477	0.5781	0.3743	0.0956	0.3223
5	SWAG $f_g = 0.8$	2400	32.88	0.4400	0.5850	0.3786	0.0849	0.3238
6	WAG	2400	30.12	0.4639	0.6435	0.3779	0.0821	0.2951

The approximately steady-state pressure drop for Experiments 4, 5 and 6 are as shown in the graphs (a) of Figures 9-11 were approximately 85 psi, 90 psi and 75 psi respectively. In Experiments 4 and 6, the oil injection rate was 1.4 cc/min instead of being 1.5 cc/min. The most likely sources of variation in the values of pressure drop are due to the small change in the injection rate and a change in the values of the absolute permeability and end point relative permeability to oil. The water production increases approximately linearly until oil breaks through. Very little water production was realized after breakthrough.

The connate water saturation values for each experiment were determined using material balance and are reported in Table 4. The end point permeability to oil at connate water saturation was determined at three rates: 1.25 cc/min, 1 cc/min and 0.75 cc/min to ascertain the consistency in end point permeability to oil during each experiment. The average end point permeabilities to oil (k_{ro}^{o}) are reported in Table 4. The variations in values of residual oil saturation and end-point water permeability are most likely due to changes in the core cleaning procedure and inherent experimental errors.

3.2.2 Secondary Imbibition (Water-Flood)

In Figures 6-11, the graph labeled as figure (b) shows the normalized oil recovery and pressure drops obtained from the data recorded during the secondary imbibition cycle. The cumulative oil recoveries were plotted as a ratio of the change in residual oil saturation after the waterflood to the residual water saturation after waterflood ($[(S_{or})_{wf} - S_o]/(S_{or})_{wf}$. The waterflood in all experiments was conducted at 1.4 cc/min, with the Rapoport and Leas (1953) scaling coefficient approximately of 8.9.

During the initial stages of water injection the pressure drop starts to build up until the water breaks through. After breakthrough, the pressure drop begins to stabilize at approximately steady state conditions at residual oil saturation. The residual oil saturations (S_{or}) were calculated for each of the experiments using material balance. The values of the approximately steady state pressure drop increases from 260 psi to 510 psi during experiments 1 and 3 respectively. This was most likely due to the drop in the values of the absolute permeability from 68.45 mD to 30.13 mD. The approximate steady state pressure drops for the remaining experiments were reasonably consistent with stable values of absolute permeability.

The end-point permeability to water (k_{rw}^{o}) at residual oil saturation was determined at three rates: 1.25 cc/min, 1 cc/min and 0.75 cc/min. The average end point relative permeability to water for each experiment is shown in Table 4. The variations observed in values of the residual oil saturation and end point permeability to water were most likely due to the change in core cleaning procedure and inherent experimental errors. The results shown in Table 4 and the graphs labeled (a) and (b) in Figures 6-11 indicate that at the end of the waterflood cycle all of the experiments were conducted under the conditions that are close to being consistent. Thus meaningful comparisons between CGI, SWAG and WAG floods should be possible.

3.2.3 Tertiary Injection Processes

Three different tertiary recovery processes (CGI, WAG and SWAG) with six different tertiary floods were investigated in this study. The objective was also to evaluate the performance of SWAG process at different values of fractional flow of gas. In addition, a comparison of the performance of CO_2 gas injection (CGI), Water-Alternating-Gas (WAG) and Simultaneous Water and Gas (SWAG) Injection was desired. Two performance indicators were chosen as the basis for the comparisons: tertiary recovery factor (TRF) and gas utilization factor (UF).

The tertiary recovery factor (TRF) is defined as the ratio of the tertiary flood residual oil saturation to the waterflood residual oil saturation.

$$TRF = \frac{(S_o)_{TF}}{(S_{or})_{wf}} \quad \text{.....(3-1)}$$

where, $(S_o)_{TF}$ – oil saturation during tertiary flood and $(S_{or})_{wf}$ – waterflood residual oil saturation.

Recovery factors are mostly affected by capillary number (N_{ca}) defined as ratio of viscous to capillary forces. In a multiphase flow through porous media with wettability alteration, one definition of the capillary number is (Lake, 1989):

$$N_{ca} = \frac{u\mu}{\sigma cos\,\theta} \quad \text{.....(3-2)}$$

where, u is the injection velocity (cm/min), μ is the viscosity of the displacing fluid (cP), σ is interfacial tension between the displacing and displaced fluid (dyne/cm) and Θ is the contact angle. In this study, the rock system had a reasonably consistent water wet state. Hence we can neglect the cosine term. Lower tertiary recovery factor values (higher recoveries) are generally associated with higher capillary numbers.

CO_2 utilization factor is commonly used to evaluate field projects and is defined as the ratio of the volume of CO_2 injected at standard conditions to stock tank barrels of oil produced (Jarell et al., 2002).

$$UF = \frac{(G_i)_{sc}}{(N_p)_{sc}} \quad \text{..... (3-3)}$$

where, $(G_i)_{sc}$ is standard cubic feet of CO_2 injected and $(N_p)_{sc}$ is cumulative stock tank barrels of oil produced.

3.2.3.1 CO_2 Solubility in Water

The solubility of CO_2 in water was briefly reviewed in this study. The concentration of CO_2 in water was reported to be in range of 1125-1400 ppm at atmospheric pressure and temperature of 20 ^oC (Fu et al., 1998). Enick and Klara (1992) correlated the effect of CO_2 solubility in brines based on concentration of total dissolved salts. Based on this (Enick and Klara, 1992) model for a 2% $CaCl_2$ brine the concentration of dissolved CO_2 was estimated to be about 1450 ppm. Formation volume factors for CO_2 saturated water were calculated as described by Klins, (1984):

$$B_w = \{\rho_{wsc} + [(R_{sw})([(M_{co2})/2130.3]\}/\rho_w \quad \text{.....(3-4)}$$

where ρ_w and ρ_{wsc} are expressed lb/ft^3, B_w is expressed in bbl/STB, R_{sw} is expressed in SCF/STB. The formation volume factor for the CO_2 saturated brine was estimated to be 1.0206 bbl/STB at a pressure of 2500 psi and it was estimated to be 1.0027 under standard conditions. The gas solubility data used for this calculation was from Klins (1984) and the density data was from Parkinson and de Nevers, (1969). However Garcia, (2001) computed density changes in CO_2 saturated NaCl brine by accounting for the changes in density both due to the salinity and solubility of CO_2. He reported a maximum of 20% increase in the density of 0.25 weight percent NaCl solution by saturating it with CO_2. The density changes in CO_2 saturated brines still

remains to be resolved and the time scales needed to attain these conditions are not well understood. In the study presented here we did not account for the density changes (if any) caused by solubility of CO_2 in 2% $CaCl_2$ brine and all the water saturation calculations were based on this assumption.

3.2.3.2 Experiment #1: Continuous CO_2 Injection

Following an initial oil and water flood, dense CO_2 was continuously injected into the core at 0.333 cc/min. The pressure drop values and normalized oil and water production were plotted as a function of the number of pore volumes of CO_2 injected and are shown in Figure 6(c). The cumulative oil produced was normalized by waterflood residual oil saturation as the ratio of change in oil saturation during the tertiary flood to the waterflood residual oil saturation ($[(S_{or})_{wf} - S_o]/(S_{or})_{wf}$) and the cumulative water produced was plotted as the ratio of change in water saturation during the flood to the water saturation prior to the tertiary flood ($[(S_w)_{wf} - S_w]/(S_w)_{wf}$).

The pressure drop across the core increases as the CO_2 phase tries to displace both water and oil. It reaches a maximum value at a time that is about half that of the initial oil response. This appears to be the process of building an oil bank. After the peak point, the pressure drops fairly rapidly until shortly after the oil and gas breaks through and the pressure drop stabilizes at an approximately steady state value. The oil and gas broke through when 0.50 and 0.52 pore volumes of CO_2 had been injected respectively. The oil production continued after the gas broke through; attaining a tertiary flood residual oil saturation of 0.0369, after 2 pore volumes of CO_2 had been injected.

The CO_2 flood recovered 89.98% of waterflood residual oil and the total recovery for the entire process was about 92.1% of the original the oil in place. At the end of the flood, the water saturation was about 0.096 and about 84.83% of the water that was present prior to the tertiary

flood was recovered. The flood performance of this experiment is shown in the first row of Table 5. The recoveries are fairly typical for miscible floods (Kulkarni and Rao, 2004).

Table 5: Summary of Tertiary Floods

Exp #	***Description***	***BP*** *(psi)*	***Injection Rate*** *(cc/min)*	$(S_{or})_{TF}$	***Tertiary Recovery*** *(ROIP)*	***Tertiary Recovery*** *(OOIP)*	***Total Recovery*** *(OOIP)*
1	CGI	2400	0.33	0.0369	0.8998	0.6340	0.9213
2	SWAG $f_g = 0.2$	2400	0.50	0.0978	0.7253	0.5008	0.8252
3	SWAG $f_g = 0.4$	2400	0.50	0.0109	0.9692	0.5787	0.9518
4	SWAG $f_g = 0.6$	2400	0.50	0.0636	0.8300	0.5231	0.8454
5	SWAG $f_g = 0.8$	2400	0.50	0.0944	0.7507	0.5076	0.8364
6	WAG	2400	0.50	0.0422	0.8602	0.4636	0.8759

3.2.3.3 Experiment #2: Simultaneous Water and Gas Injection with $f_g = 0.2$

The tertiary flooding employed during this experiment was simultaneous injection of water and gas with a gas fractional flow of 0.2. Brine (2% $CaCl_2$) and CO_2 were simultaneously injected into the core after waterflooding it, to residual oil saturation. The total injection rate was 0.5 cc/min, with CO_2 injected at 0.1 cc/min. The flow of CO_2 and brine joins at a T-junction and subsequently flows through a 2 μm filter.

As the mixture of brine and CO_2 displaces the residual oil and brine, the pressure drop across the core builds to a level significantly higher than that seen during continuous gas injection. At about the time of first oil and water production an approximately steady state pressure drop was reached. The pressure drop values and the normalized oil and water production were plotted as functions of the number of pore volumes of CO_2 injected which is shown in Figure 7(c). As discussed in Section 3.2.3.1, the approximately 15 psi change in the pressure drop observed during the experiment at about 1.2 pore volumes of CO_2 injection was

because the annulus pressure built up to a level higher than the desired value. To compensate the pressure was bled off. This pressure bleed off did not seem to impact recovery significantly, as there was no change in the recovery curve observed. The breakthroughs of oil and gas were observed at 0.17 and 0.19 pore volumes of CO_2 injected. The early breakthrough was most likely due to the higher fraction of injected water, which blocked the gas path by increasing the gas pressure. As the pressure reached a limiting point the gas created a path to flow, until the pressure dropped to a point where water blocked it again, similar to observations made in a single 2-Dimensional fracture (Persoff and Pruess, 1995). The oil was produced intermittently.

After 2 pore volumes of CO_2 had been injected, 72.53% of the waterflood residual oil was recovered. The total recovery for this experiment was calculated to be 82.52% of the original oil in place. Here CO_2 was unable to contact as much of the residual oil as compared continuous gas injection process, presumably due to water blocking. The water recovery reached at maximum value of about 46.19% at about the same time when gas broke through. After breakthrough, the water saturation in the core steadily increased with some noticeable cycling. This process eventually recovered about 26.98% of water that was present prior to the tertiary flood corresponding to a water saturation of 0.4496. Results from this experiment are tabulated in the second row of Table 5. The pressure drop was considerably higher than the CGI case and was fairly steady in contrast to the WAG results to be presented later. This indicates that the SWAG technique may be an effective mitigation technique for poor sweep efficiency.

3.2.3.4 Experiment #3: Simultaneous Water and Gas Injection with f_g= 0.4

Here the simultaneous water and gas (SWAG) injection scheme was employed at a total injection rate of 0.50 cc/min with CO_2 injection rate of 0.20 cc/min. As the mixture of brine and CO_2 displaced the residual oil and brine, the pressure drop reached the highest of the values observed during SWAG floods performed in this study. At about the time of first oil production an

approximately steady state pressure drop was reached. The pressure fluctuations were more pronounced than that observed in any of the other cases. The pressure drop values and the normalized oil and water productions were plotted as a function of pore volumes of CO_2 injected and are shown in Figure 8(c). The oil and CO_2 broke through when about 0.20 and 0.23 pore volumes of CO_2 had been injected respectively. After 2 pore volumes of CO_2 was injected 96.92% of the water flood residual oil was recovered. This process eventually recovered about 42.02% of water that was present prior to the tertiary flood, which resulted in a water saturation of 0.3782. Results from this experiment are tabulated in the third row of Table 5. The mechanism of oil recovery was similar to the SWAG with gas fractional flow of 0.2. However the highest pressure drop along with the highest cycling in pressure data was observed in this experiment which is the most likely explanation for this experiment attaining the highest recovery of the SWAG experiments.

3.2.3.5 Experiment #4: Simultaneous Water and Gas Injection with f_g= 0.6

In this experiment SWAG was injected at a gas fractional flow value of 0.6 into the core at waterflood residual oil saturation of 0.3743. A total injection rate of 0.50 cc/min was used. The pressure drop values and normalized oil and water production were plotted as a function of pore volumes of CO_2 injected in Figure 9(c), as discussed in Section 3.2.3.1. As the mixture of CO_2 and brine displaced the residual oil and brine, the pressure drop across the core was built to a level higher than CGI and a little lower than that observed in SWAG with f_g= 0.2. At about the time of first oil production the system began to attain an approximately steady state pressure drop. The water recovery curve had two linear trends, the first linear trend changes approximately at the same time when the significant decrease in pressure drop was observed. The first trend was observed when the initial water was produced and the second linear trend started when the injected water was first seen in the effluent. The oil and gas broke through when

0.24 and 0.34 pore volume of CO_2 had been injected respectively. After 2 pore volumes of CO_2 was injected, the residual oil saturation in the core was reduced to 0.0640 with tertiary flood oil recovery of 83.00% of the residual oil in place. This is lower than the results from CGI and SWAG with f_g= 0.4 but higher than the results from SWAG a gas fractional flow value of 0.2 This process recovered about 73.59% of water that was present prior to the tertiary flood, which resulted in a water saturation of 0.1652. The results from this experiment are shown in the fourth row of Table 5.

3.2.3.6 Experiment #5: Simultaneous Water and Gas Injection with f_g= 0.8

In this experiment SWAG was injected at a gas fractional flow value of 0.8 with a total injection rate of 0.50 cc/min. As the mixture of CO_2 and brine displaced the residual oil and brine, the pressure drop across the core built to a level similar to what was observed in the SWAG with a gas fractional flow value of 0.2. At about the time of first oil production an approximately steady state pressure drop was reached. The pressure drop values and the normalized oil and water production are plotted as a function of pore volumes of CO_2 injected in Figure 10(c). After breakthrough the water recoveries followed an approximately linear trend until approximately one pore volume of CO_2 had been injected. After this pore volume of CO_2 was injected the water recovery has another approximate linear slope corresponding to the production of initial and injected water respectively.

The normalized water recovery was linear approximately until the time the pressure drop values begin to decline. The oil and gas broke through when 0.41 and 0.42 pore volumes of CO_2 had been injected respectively. This oil bank produced a substantial amount of oil at breakthrough. The oil production continued with smaller quantities of oil after breakthrough. The pressure fluctuations did not occur as frequently as observed in earlier experiments most likely due to the higher gas fraction, avoiding the blocking of gas flow. This is also the likely

explanation for the steady state pressure drop being lower than that observed by the results for SWAG with gas fractional flow value of 0.2. After 2 pore volumes of CO_2 have been injected the tertiary oil recovery was about 75.07% of the residual oil in place which was similar to the results observed with SWAG at a gas fractional flow value of 0.2. This process recovered about 86.47% of water that was present prior to the tertiary flood resulting in a water saturation of 0.0841. The water recoveries tend to match that of the CGI flood closely. Results from this experiment are shown in the fifth row of Table 5.

3.2.3.7 Experiment #6: Water Alternating Gas Injection

In this experiment a 1:1 WAG injection was conducted in a core at residual oil saturation of 0.4639 and with a slug size of 0.25 PV. The gas and water were injected alternatively one after the other instead of simultaneous injection. The total injection rate of 0.50 cc/min was used. At first a CO_2 slug displaced the residual oil and brine followed by an equal size slug of water and the sequence continued until about 2 pore volumes of CO_2 were injected. The pressure drop values and normalized oil and water production were plotted as functions of pore volumes of CO_2 injected in Figure 11(c). The pressure drop across the core started to build until the oil broke through. The build-up and decline (pressure cycling) observed in the pressure drop was in response to the arrival of CO_2 and water slugs respectively. The oil production was approximately linear until about 0.70 pore volumes of total injection, followed by series of oil production and plateau periods. The water production was characterized by a series of linear production followed by plateau periods (production of CO_2 only). Miscible WAG recovered 86.02% of residual oil in place after about 2 pore volumes of CO_2 had been injected. However when SWAG works it does not have plateau periods like WAG. The normalized water recovery during WAG process fluctuated between an approximate high value of 0.75 and low value of about 0.50. Results from this experiment are tabulated in the sixth row of Table 5.

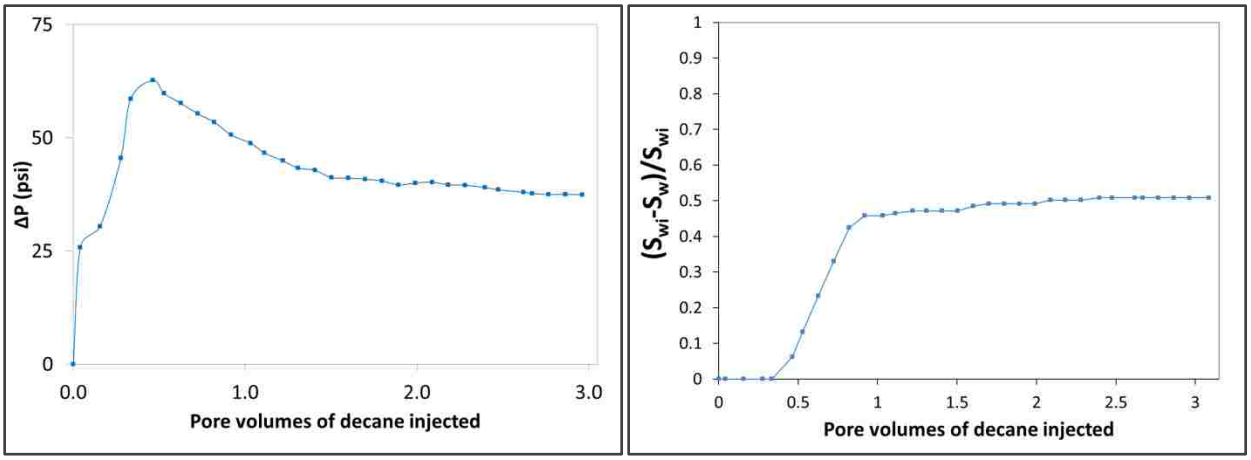

(a) Oil Flood with n-Decane

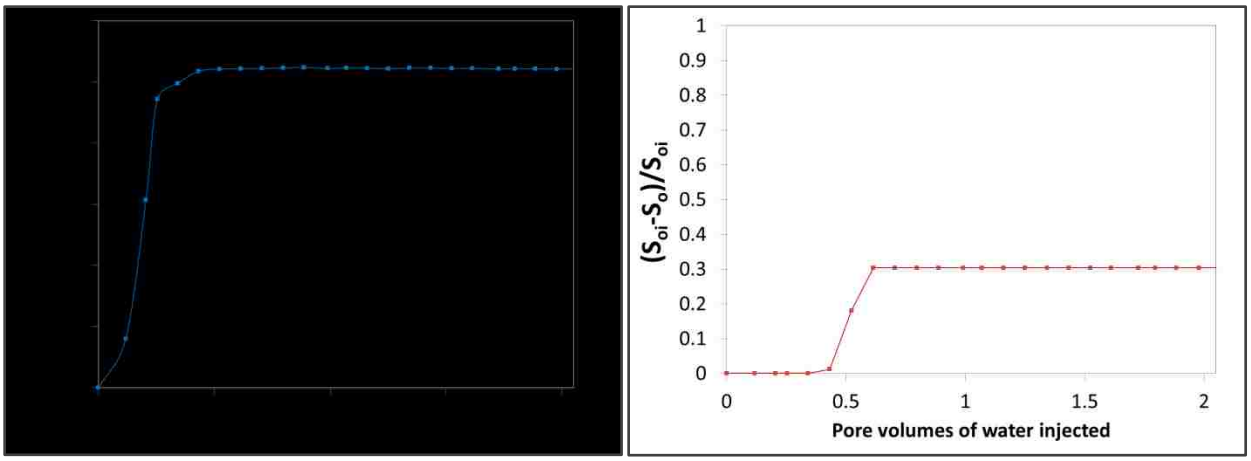

(b)Waterflood with 2% $CaCl_2$ Brine

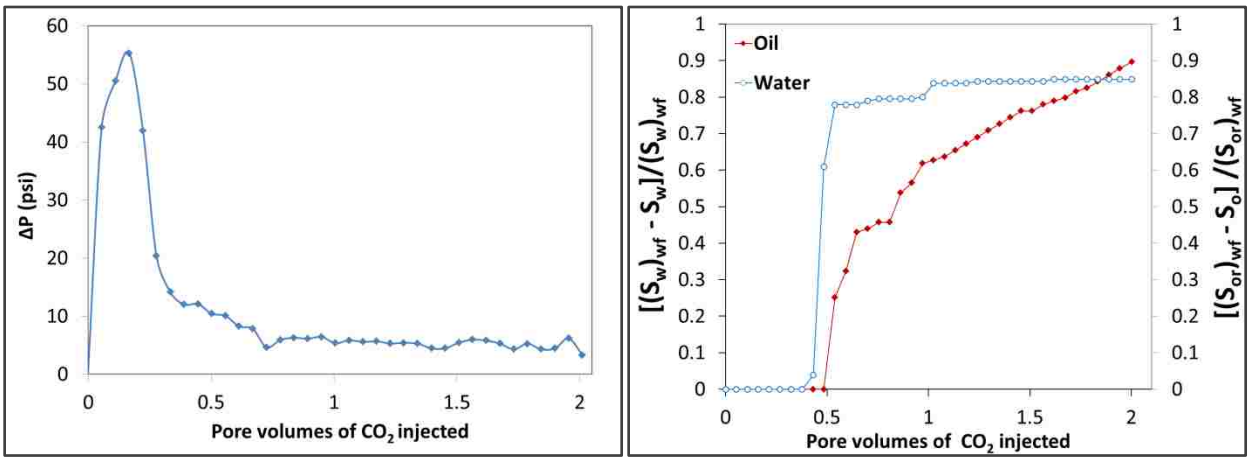

(c) Tertiary Flood with Continuous Miscible CO_2 Injection

Figure 5: Experiment #1: Continuous Gas Injection using CO_2

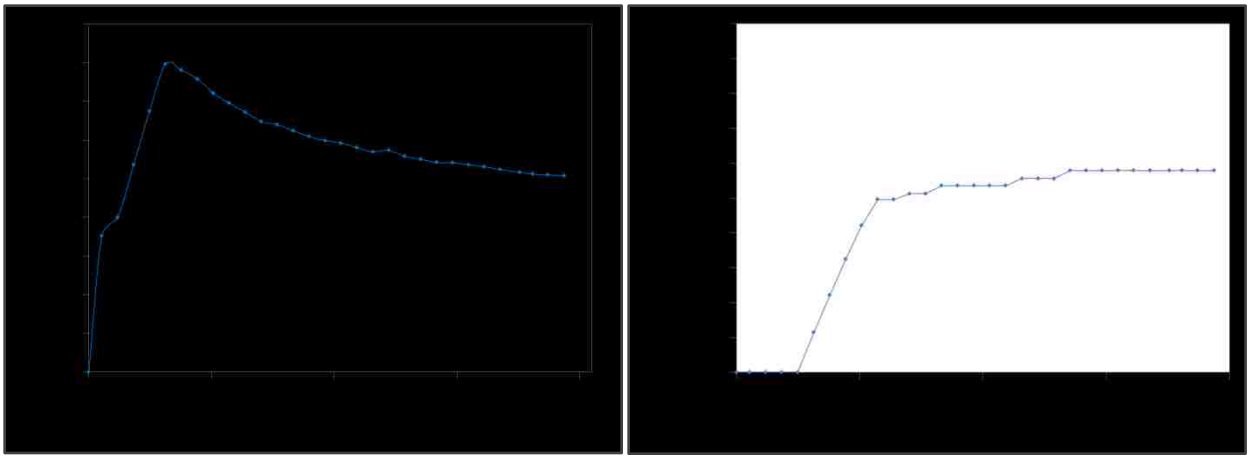

(a) Oil Flood with n-Decane

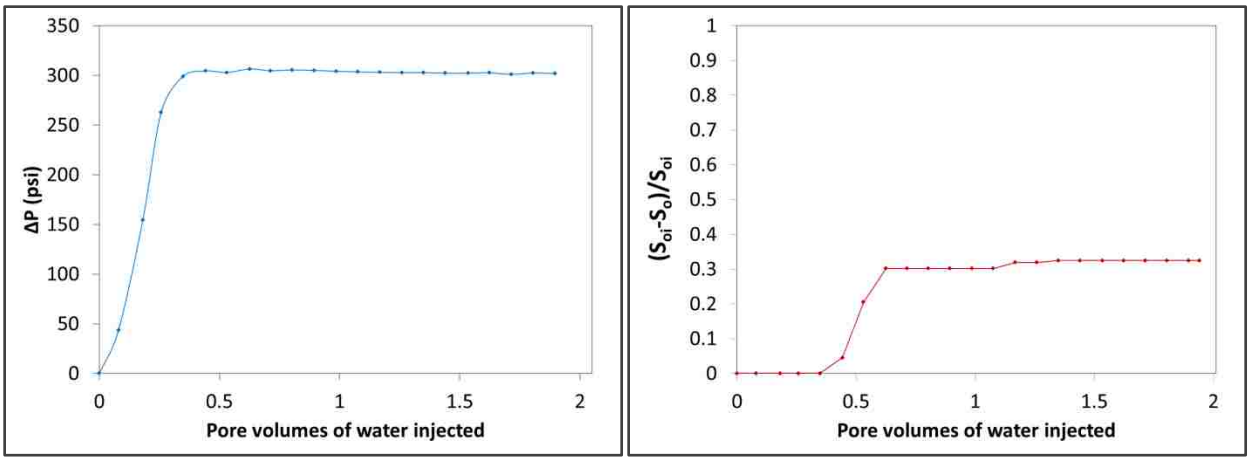

(b)Waterflood with 2% $CaCl_2$ Brine

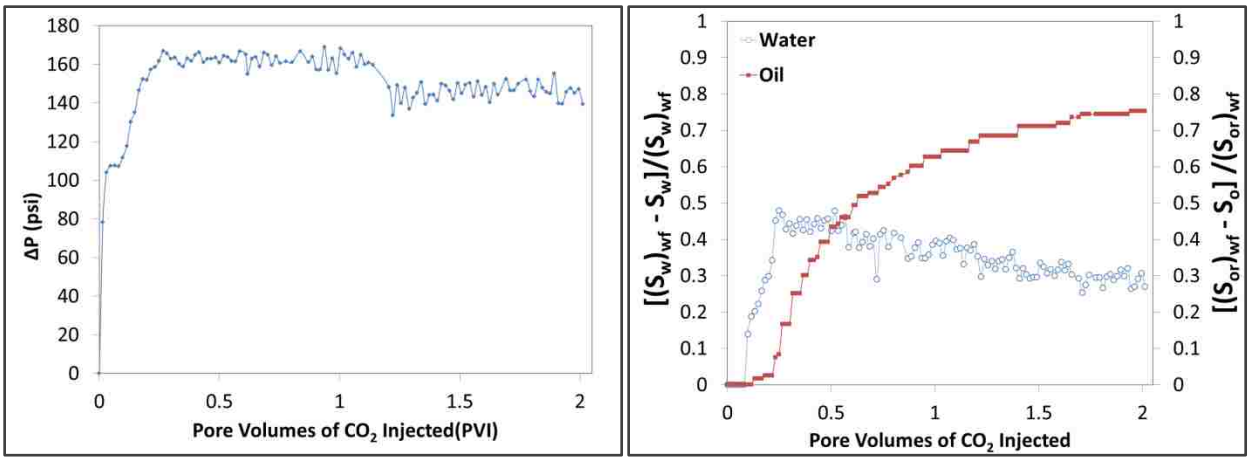

(c) Tertiary Flood with Miscible SWAG (f_g=0.2) Flood using CO_2

Figure 6: Experiment #2: Miscible SWAG Injection with f_g= 0.2 using CO_2

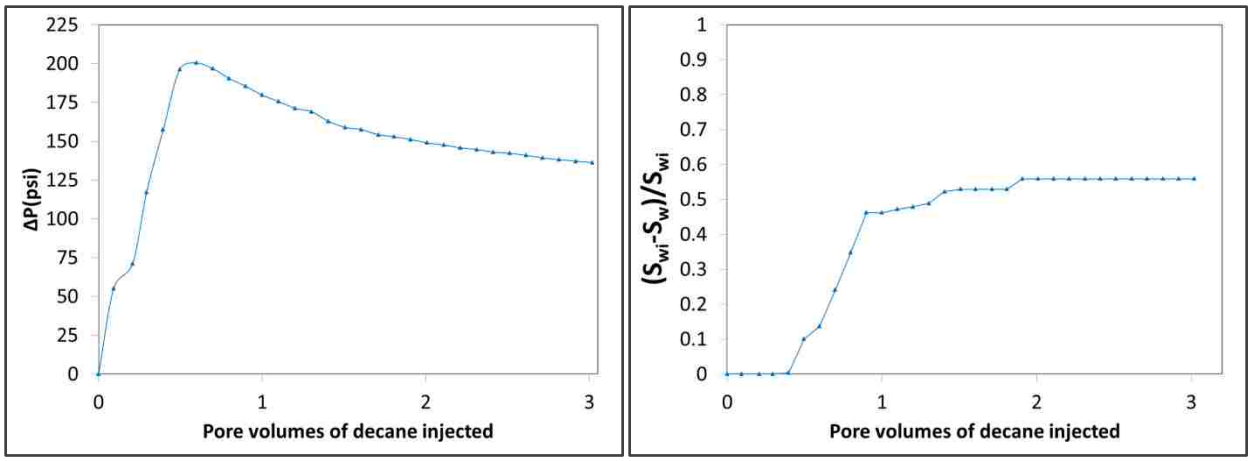

(a) Oil Flood with n-Decane

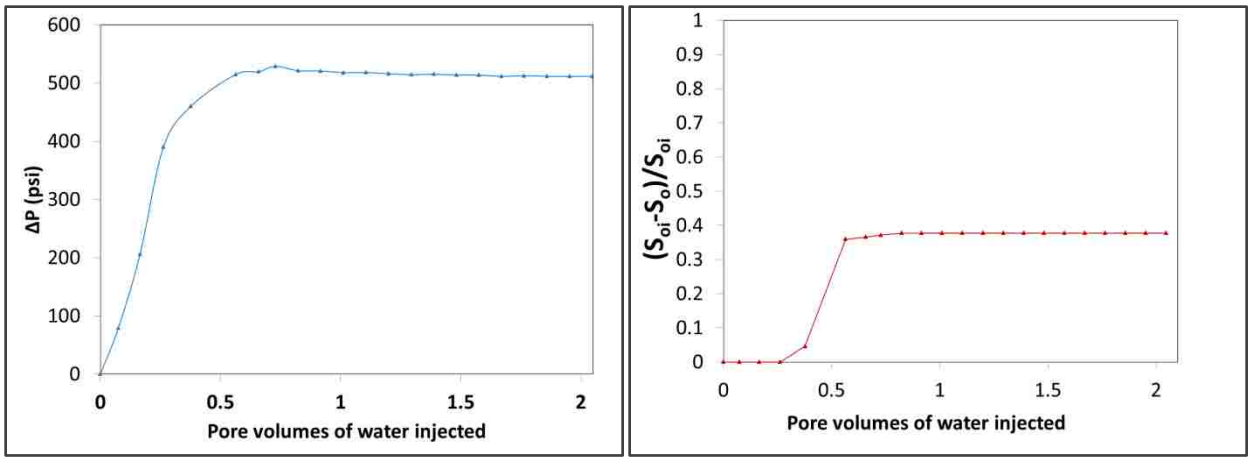

(b)Waterflood with 2% $CaCl_2$ Brine

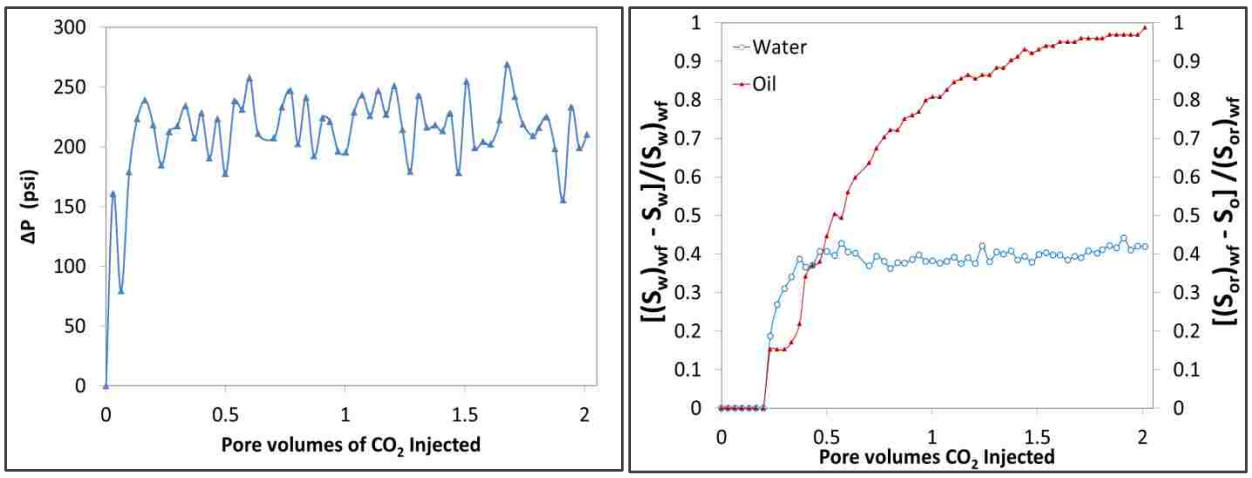

(c) Tertiary Flood with Miscible SWAG (f_g=0.4) Flood using CO_2

Figure 7: Experiment #3: Miscible SWAG Injection with f_g = 0.4 using CO_2

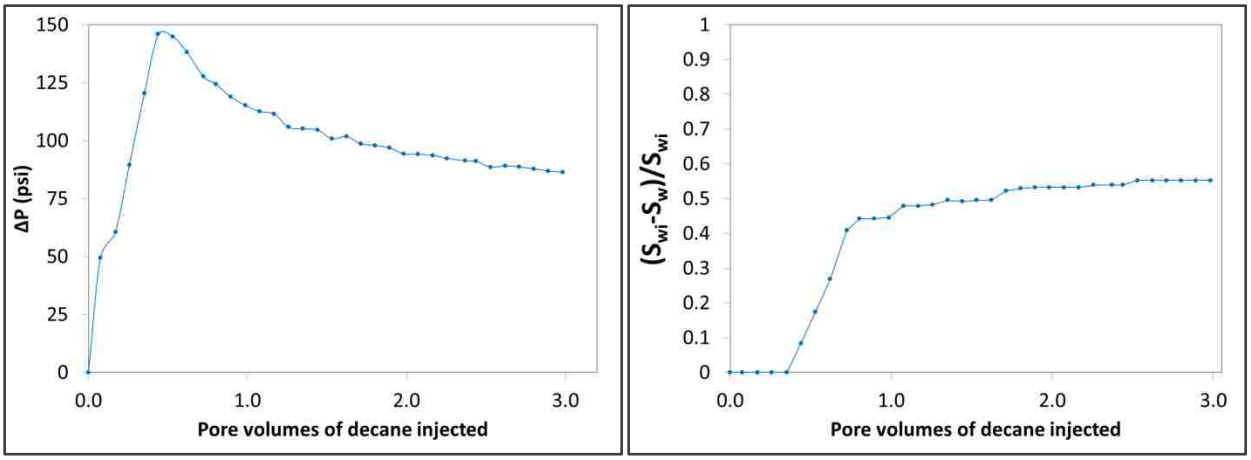

(a) Oil Flood with n-Decane

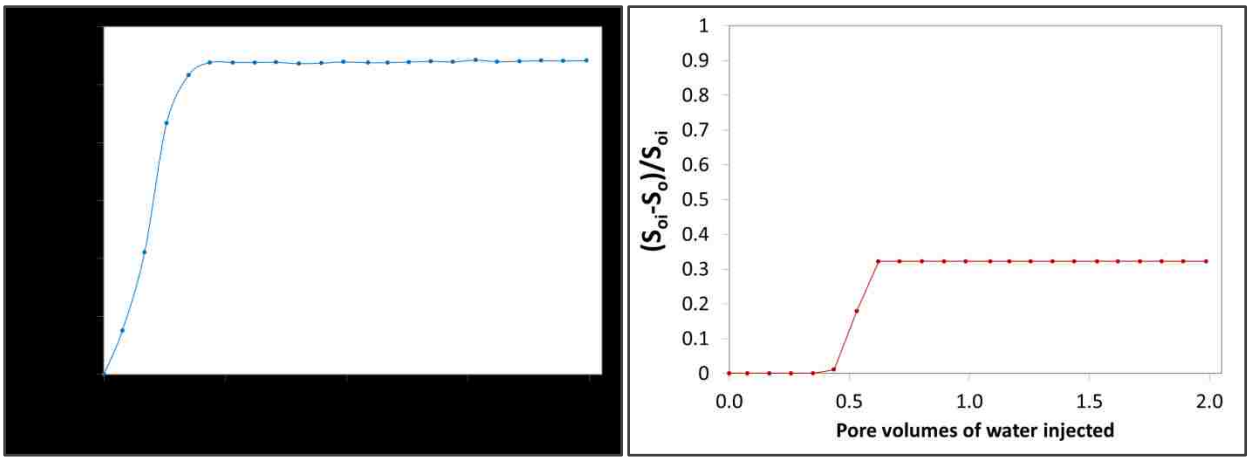

(b)Waterflood with 2% $CaCl_2$ Brine

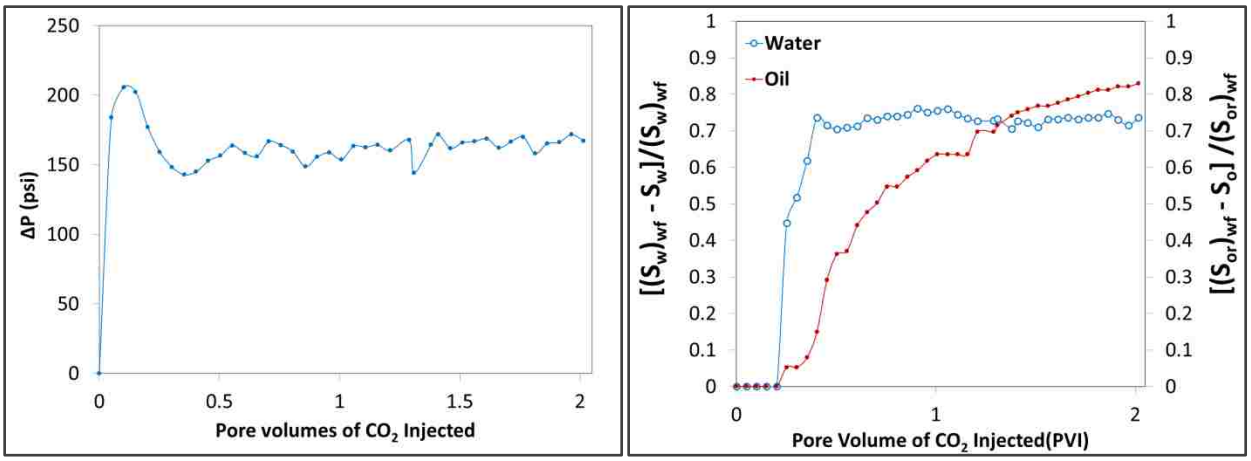

(c) Tertiary Flood with Miscible SWAG (f_g=0.6) Flood using CO_2

Figure 8: Experiment #4: Miscible SWAG injection with f_g = 0.6 using CO_2

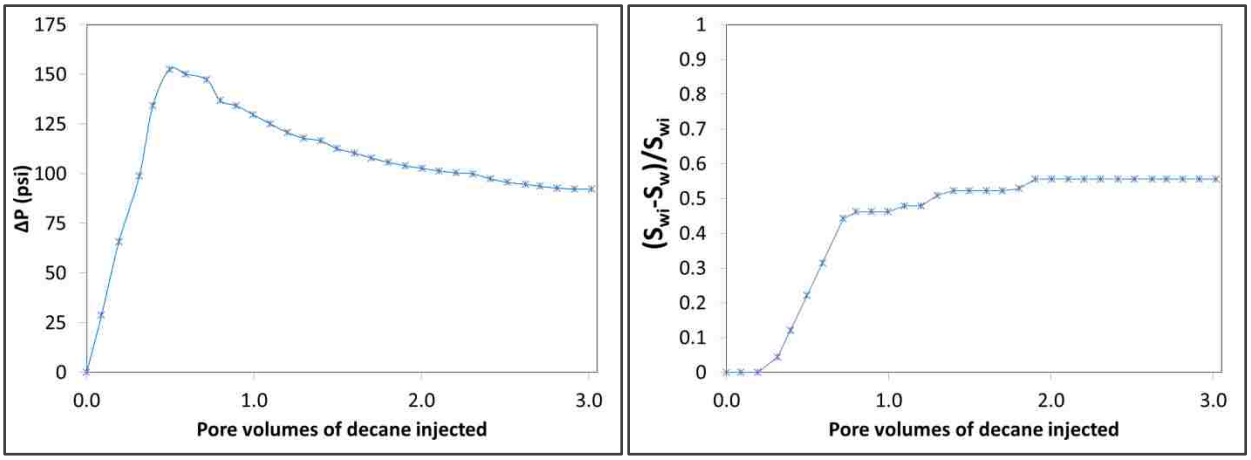

(a) Oil Flood with n-Decane

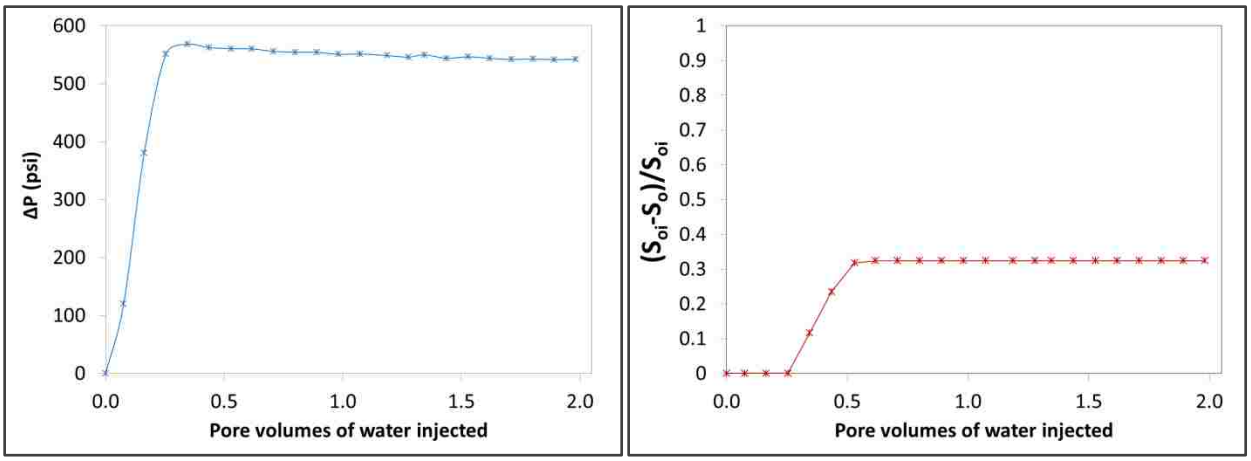

(b)Waterflood with 2% $CaCl_2$ Brine

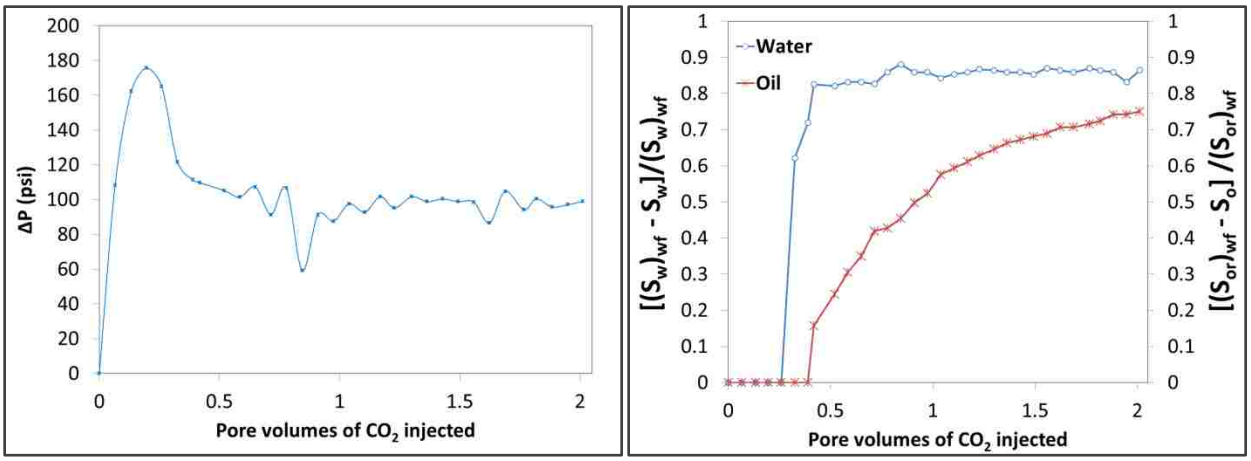

(c) Tertiary Flood with Miscible SWAG (f_g=0.8) Flood using CO_2

Figure 9: Experiment #5- Miscible SWAG Injection with f_g = 0.8 using CO_2

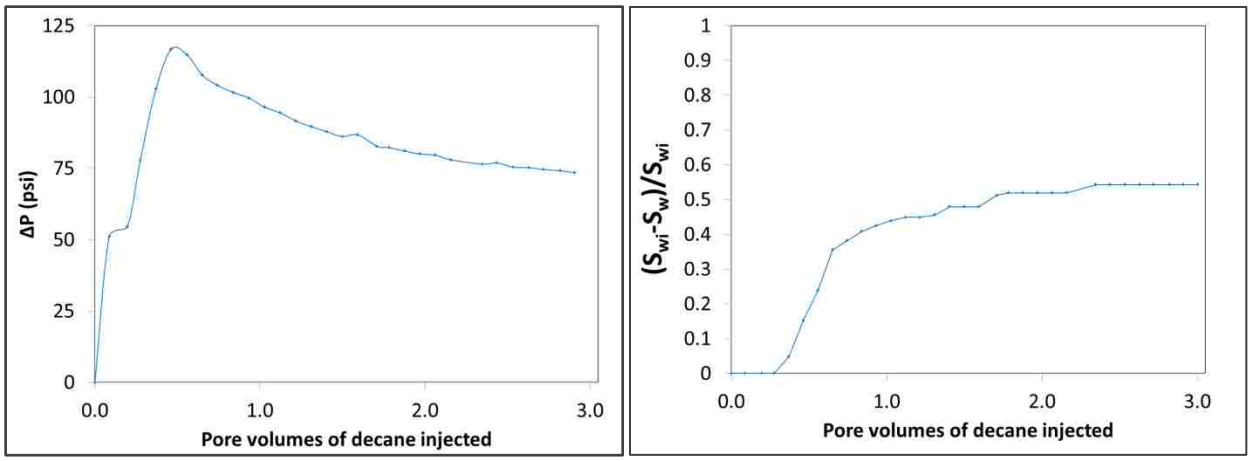

(a) Oil Flood with n-Decane

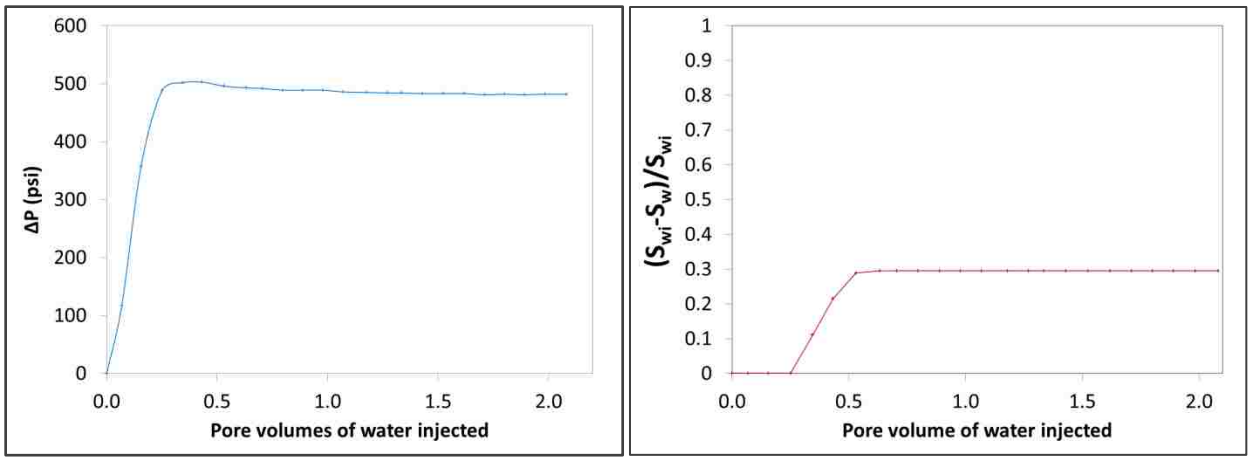

(b)Waterflood with 2 % $CaCl_2$ brine

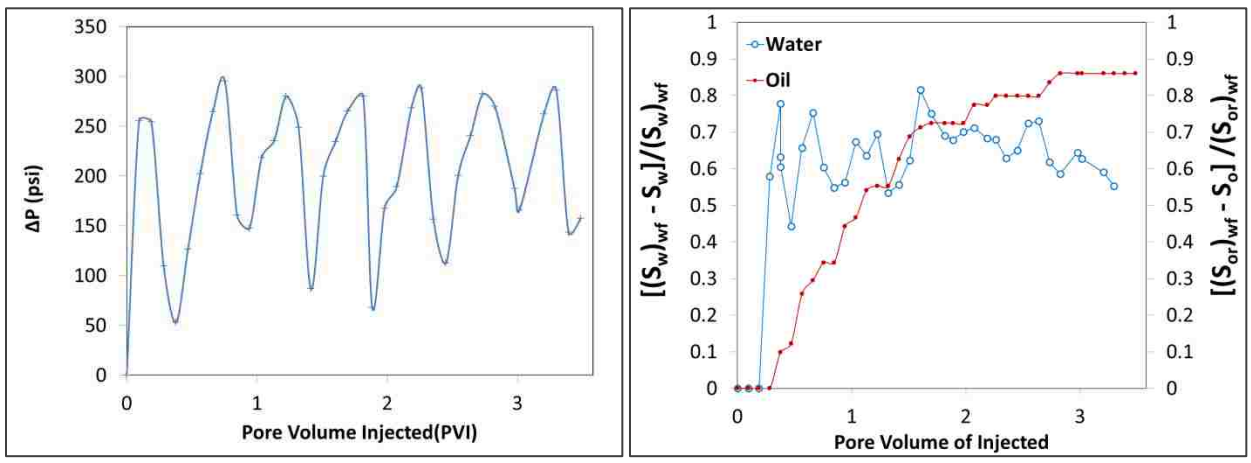

(b) Tertiary Flood with Miscible WAG

Figure 10: Experiment #6: Miscible WAG (1:1) Injection with Slug Size of 0.25 using CO_2

3.3 Discussion

This section discusses the effect of fractional flow of gas (f_g) values on the pressure drop, mobility, tertiary recovery factor and gas utilization factor.

3.3.1 Effect of Fractional Flow of CO_2 on Pressure Drop

At a constant total injection rate of 0.5 cc/min, the fractional flow of gas was increased in steps of 0.2 with every experiment. When the fractional flow of CO_2 was increased from 0.2 to 0.4 the approximately steady-state average pressure drop across the core increased from 160 psi to a maximum of 250 psi with 50 psi variations. Further increasing the f_g value to 0.6 decreased the average pressure drop back down to 160 psi, a level equivalent to that observed at f_g = 0.2. At f_g value of 0.8, the approximately steady state average pressure drop across the core decreases further to a value of 100 psi.

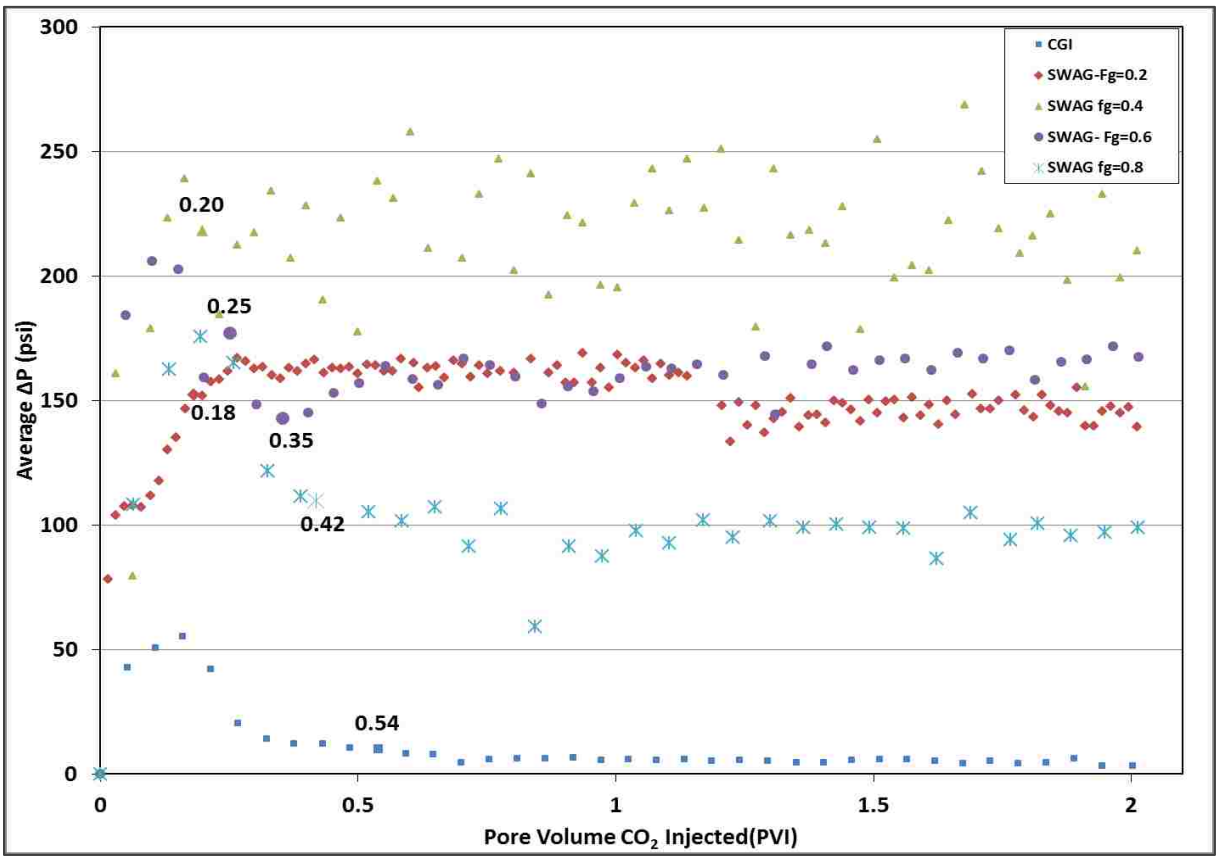

Figure 11: Effect of Fractional Flow of CO_2 on Average Transient Pressure Drop

This behavior may be analogous to the two distinct flow regimes concept (the high quality regime and the low quality regime) for foam flow through porous media. This phenomenon was observed for a wide variety of porous media, surfactants, and injection rates (Alvarez et al., 2001). The contour plot of nitrogen foam flow in porous media in the absence of oil is shown in Figure 13. The high quality regime (f_g>0.94) is shown in the left had side and the low quality regime (f_g<0.94) is on the right hand side. In the high quality regime the pressure contour lines are almost vertical which means steady state pressure gradients are reasonably independent of gas flow rates (but mostly dependent on the liquid flow rate) and in the low quality regime the pressure contours are horizontal which means the steady state pressure gradient are reasonably independent of liquid flow rate (but mostly dependent on gas flow rate).

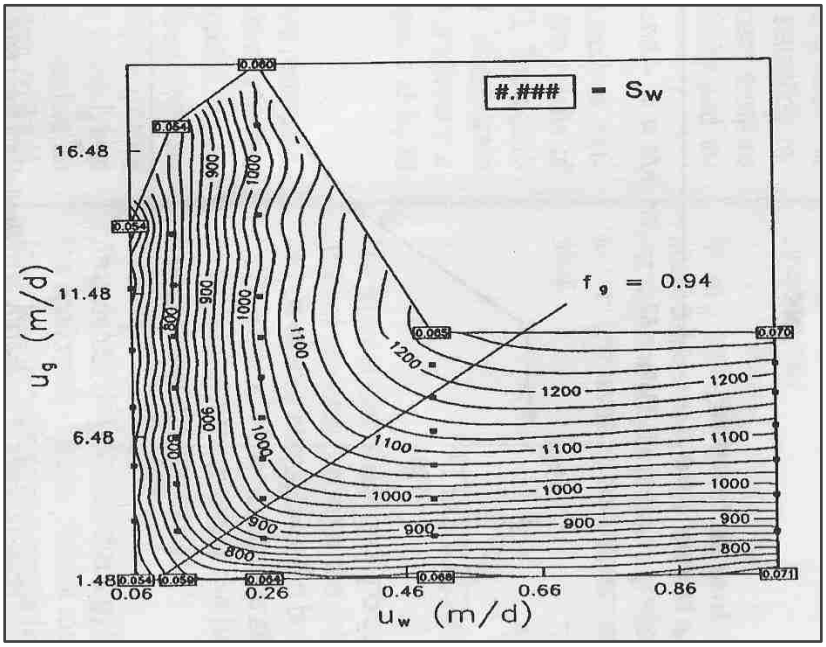

Figure 12: High and Low Quality Regimes for N_2-foams (Osterloh and Jante, 1992)

In the experiments presented here the fractional flow of CO_2 is increased from 0.2 to 0.4 (increasing gas flow rate from 0.1 cc/min to 0.2 cc/min), the transient state pressure drop increased in a manner similar to the response seen in foam flow in the low quality regime. With a

further increase in the fractional flow of CO_2 the average pressure drop decreased in response to a decrease in the water flow rate. In foams, transition from one flow regime to another occurs at a limiting capillary pressure value (P_c^*) corresponding to a fractional flow of gas value denoted by f_g^*. We did not use any surfactant in our experiments nor did we observe any foam in the effluent, moreover in our experiments oil was also flowing. In our experiments it is not clear what might be causing this behavior.

The pressure response during SWAG injection at immobile oil saturation post the tertiary recovery process seems to have the two flow regime behavior. The change in average pressure drop as a function of f_g at a total injection rate of 0.3 cc/min (corresponding to a superficial velocity of 0.0592 cm/min) is plotted in Figure 13. Chang and Grigg (1999) conducted experiments on simultaneous injection of CO_2 and brine and observed that at gas fractional flow values less than 0.333, the pressure drop across the core increased with increasing gas fractional flow, while at gas fractional flow values higher than 0.333, the pressure drop decreased with increases in the fractional flow of gas. Our experiments behaved similarly with a transition somewhere around $f_g = 0.4$ as shown in Figure 14.

3.3.2 Effect of Fractional Flow on Mobility

Chang and Grigg (1999) made a simplifying assumption that foam behaved as a single fluid and the defined total mobility of foam as the ratio of total superficial velocity to the average pressure gradient which was equal to the ratio of the effective permeability to the effective viscosity expressed as mD/cP. Similarly we assumed the water and CO_2 mixture as single fluid and calculated the value of mobility as function of f_g. The plot of mobility vs. gas fractional flow is shown in Figure 14. At $f_g = 0.4$ the value of the mobility is a minimum and a step increase or decrease in the fractional flow of CO_2 caused increase in the values of the calculated mobility.

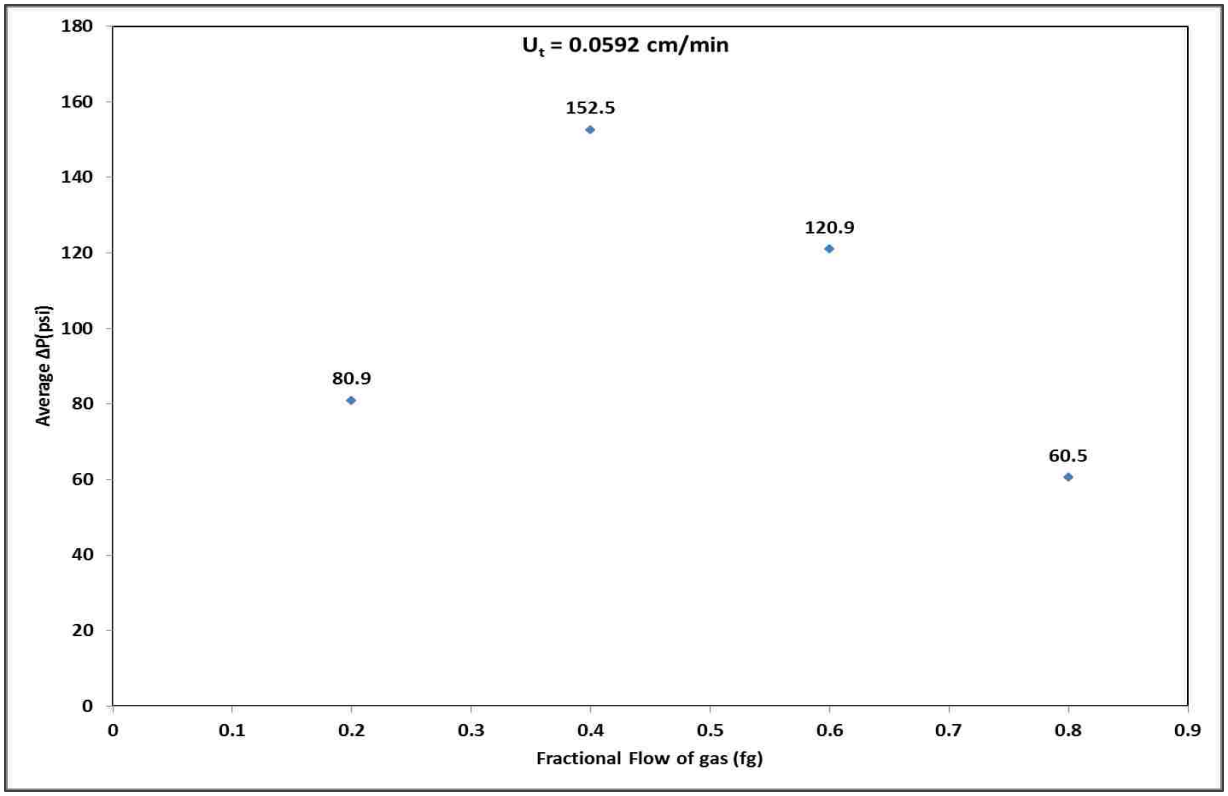

Figure 13: Effect of Fractional Flow of CO_2 on Average Steady State Pressure Drop

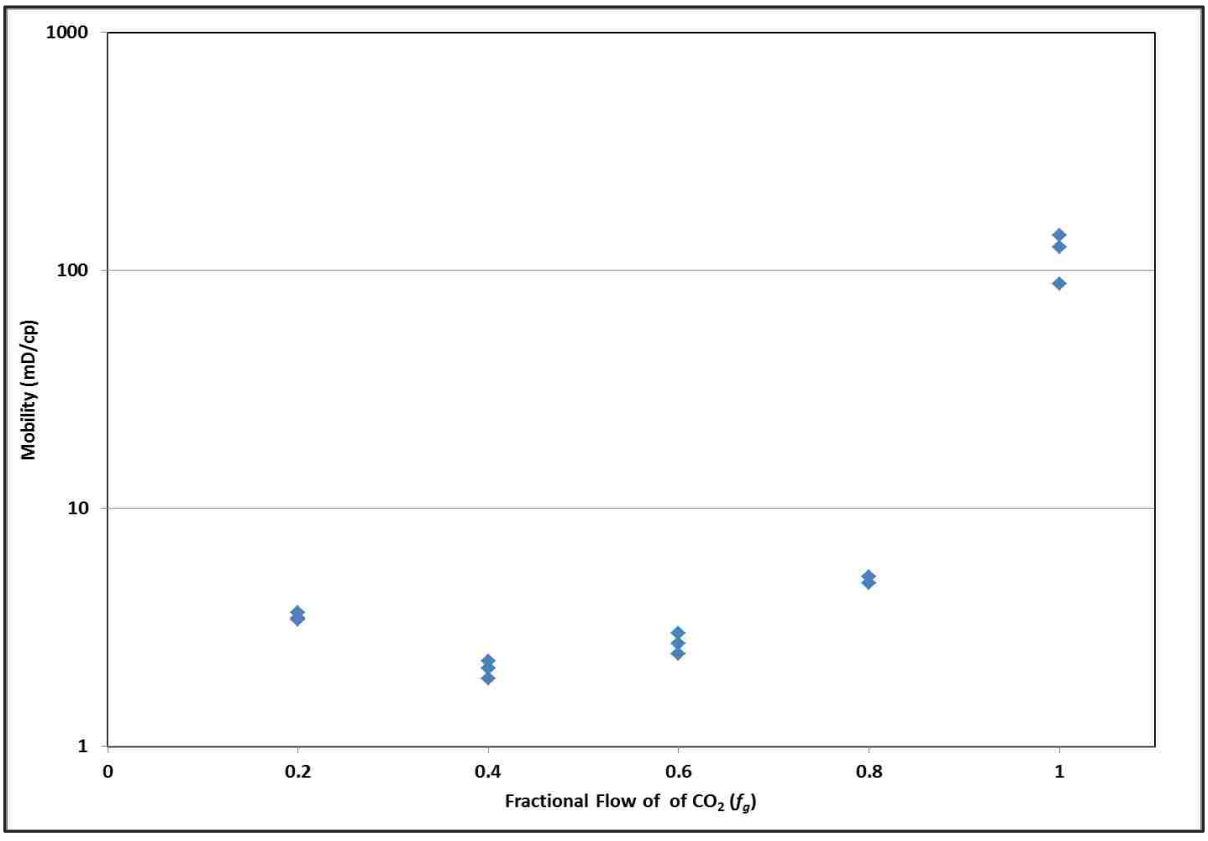

Figure 14: Effect of Fractional Flow of CO_2 on Mobility

3.3.3 Effect of Fractional Flow of CO_2 on Tertiary Recovery Factor

As discussed in section 3.2.3, lower tertiary recovery factors (higher total recoveries) are associated with higher capillary numbers. The tertiary recovery factors are plotted as function of pore volumes of CO_2 injected in Figure 15 and a graph of tertiary recovery factor versus total pore volumes injected is provided in Appendix B.

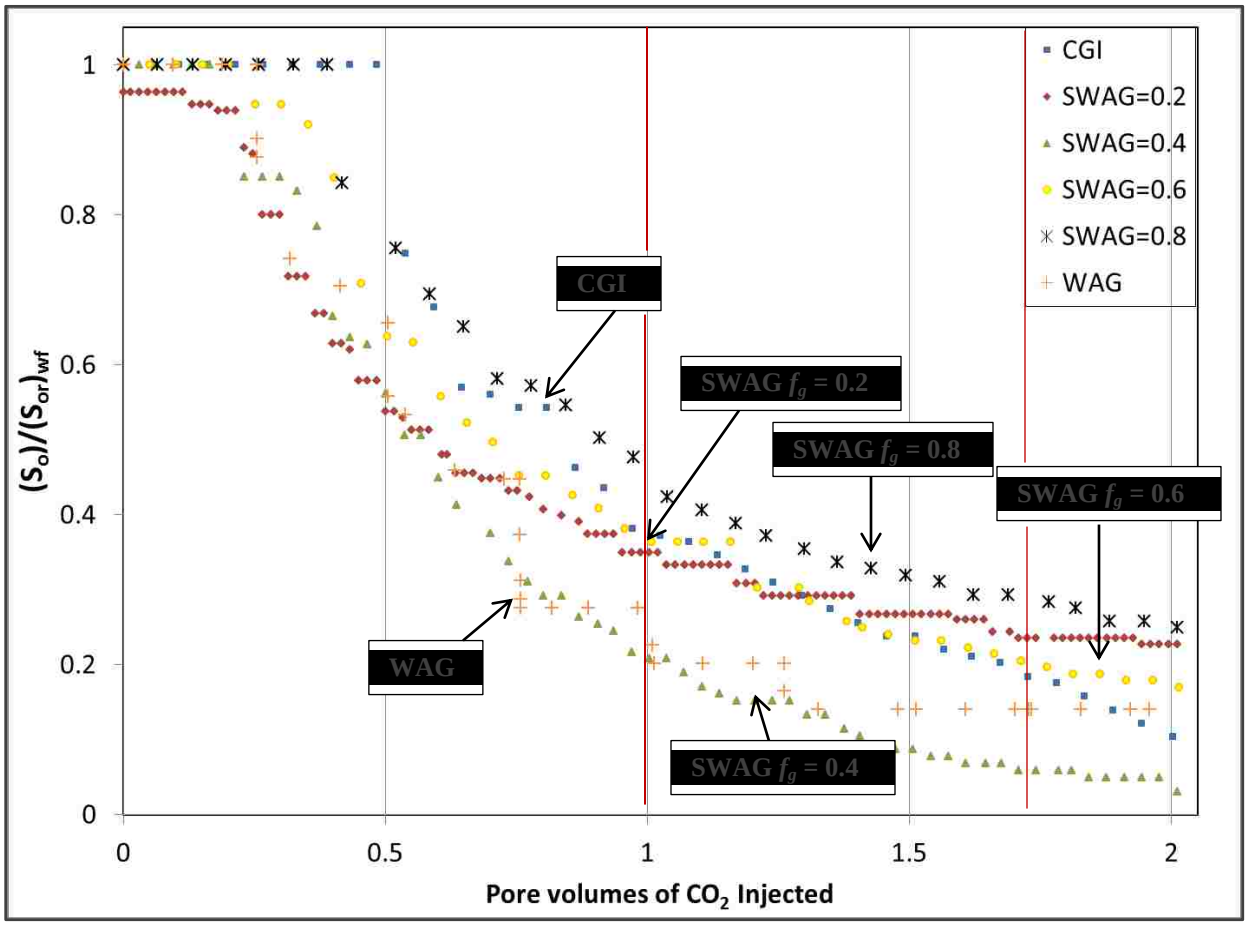

Figure 15: Comparison Tertiary Recovery Factor over 2 Pore Volumes of CO_2 Injected

Highest recoveries were obtained with SWAG at f_g =0.4, followed by CGI and SWAG at f_g = 0.6 and WAG floods after 2 pore volumes of CO_2 had been injected. The lowest recoveries were achieved by SWAG floods with f_g value of 0.8. The recoveries achieved by SWAG at f_g =

0.4 and continuous gas injection (CGI) are comparable but higher recoveries were achieved by SWAG with $f_g = 0.4$.

The CGI process has a sharp, almost piston-like breakthrough followed by long rarefaction. The SWAG flood with $f_g = 0.8$ has similar behavior but tapers off to very inefficient recovery after about a pore volume injected. The rest have recoveries that have much smaller piston-like displacements but with somewhat stronger rarefaction waves. All of the SWAG floods except $f_g = 0.8$ and the WAG flood have better recovery values than CGI until about 1.3 pore volumes of CO_2 have been injected.

The recoveries by WAG was more pronounced compared to CGI until about 1.9 pore volumes of CO_2 was injected. WAG was able to mobilize more residual oil during the piston-like breakthrough compared to CGI. The characteristic WAG-plateaus can be observed in Figure 16. In continuous gas injection floods the recovery is due to miscible interaction between the gas and the contacted oil. But in SWAG the recoveries are a result of the combined effect of CO_2 contact and an increase in the effective viscosity. Hence SWAG with $f_g = 0.4$ had an optimum combined effect (i.e., miscibility and contact) resulting in the highest tertiary recovery after 2 pore volumes of CO_2 was injected. The recoveries by the tertiary floods relative to SWAG with $f_g = 0.4$ are shown in Table 6.

Table 6: Comparison of Tertiary Recovery Factor

Experiment	TRF after 2PV CO_2 Injected	Ratio $(TRF)/(TRF)_{fg=0.4}$
CGI. f_g =1	0.8998	0.9284
SWAG f_g =0.2	0.7253	0.7483
SWAG f_g =0.4	0.9692	1
SWAG f_g =0.6	0.8330	0.8594
SWAG f_g =0.8	0.7507	0.7746
WAG	0.8602	0.8875

3.3.4 Effect of Fractional Flow of Gas on Water Recovery

The ratio of change in water saturation to the water saturation at the beginning of the tertiary flood is the measure of water recovery during the flood. The water recovery factor is plotted against the pore volumes of CO_2 injected as shown in Figure 16, for all the SWAG floods. Higher ratios mean higher water recovery and lower water saturation in the core.

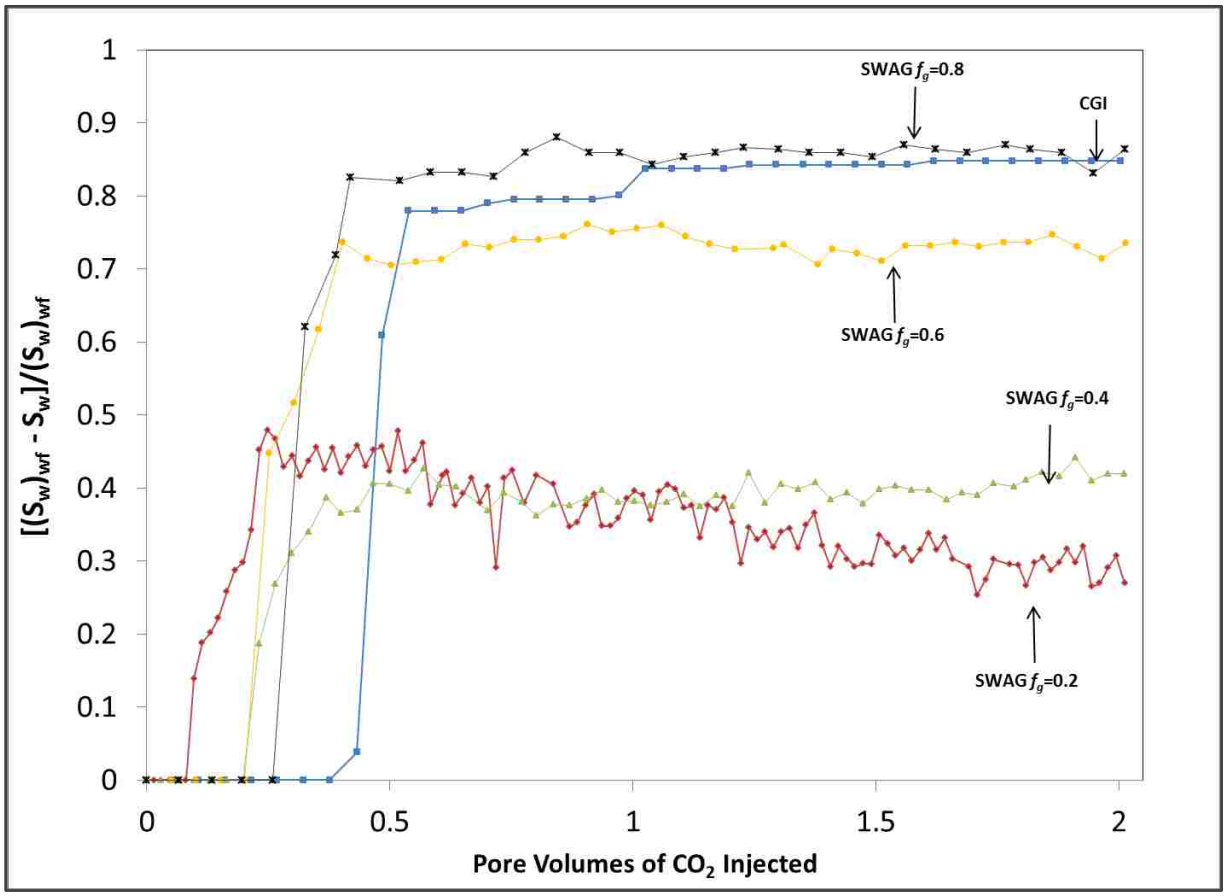

Figure 16: Comparison of Water Recovery Factor over 2 Pore Volumes of CO_2 Injected

In the SWAG process with f_g = 0.2, water breaks through at about 0.1 pore volumes of CO_2 injected. The initial water was produced until about 0.3 pore volumes of CO_2 was injected. At later time the injected water was produced. After about 0.5 pore volumes of CO_2 injected, the water recovery factors declined continually and cycled between 0.5 and 0.3. The response was most likely due to the intermittent gas blocking and resulting intermittent higher and lower water

saturations observed. The final water recovery was about 27% of the water that was present at the beginning of the tertiary flood with a corresponding water saturation of about 0.4416

In the SWAG process with f_g = 0.4, the breakthrough times of initial and injected water were observed at about 0.25 and 0.4 pore volume of CO_2 injected respectively. A less pronounced cycling in water saturations leading to smaller fluctuations in water recovery factor was also observed. However no declining trend in recovery factor or increasing trend in water saturation was observed as seen in the SWAG process with f_g = 0.2. This process recovered about 42.00% of the water that was present in the core at the beginning of this tertiary flood corresponding to a final water saturation of about 0.3781

During the SWAG process with f_g = 0.6, the breakthrough time was similar to that observed in SWAG floods with f_g = 0.4, which was about 0.25 pore volumes of CO_2 injected The water recoveries are higher after the initial water broke through compared to the experiments already discussed; recovering about 73.59% of the water that was in the core at the beginning of the tertiary flood. This was most probably due to the higher fractional flow of gas. The fluctuation in the water recovery factors are least pronounced. The final water saturation in the core was about 0.1652.

During the SWAG flood with f_g = 0.8, the breakthrough time was about 0.5 pore volumes of CO_2 injected leading to a water recovery factor of about 82.56% of water that was present at the beginning of this tertiary flood. The fluctuation in water saturation almost disappeared after about a pore volume of CO_2 was injected. The most likely reason for this response was the gas and water flow paths mostly did not interfere with each other. This process eventually recovered about 86.46% of the water that was present at the beginning of this tertiary flood resulting in a final water saturation of 0.0841. In the CGI flood a similar response was observed with an exception of slightly delayed breakthrough at about 0.5 pore volumes of CO_2 injected. During

this process, some water production was realized at about 0.9 pore volumes injected. After that almost no water recoveries were observed. The CGI process eventually recovered about 84.82% of the water that was present at the beginning of this tertiary flood resulting in a water saturation of 0.0958. The water saturation after CGI and SWAG with f_g = 0.8 floods are comparable with a little higher water saturation in the core after the CGI flood.

3.3.5 Gas Utilization Factor

The cumulative gas utilization factor for all the experiments are plotted in Figure 17.

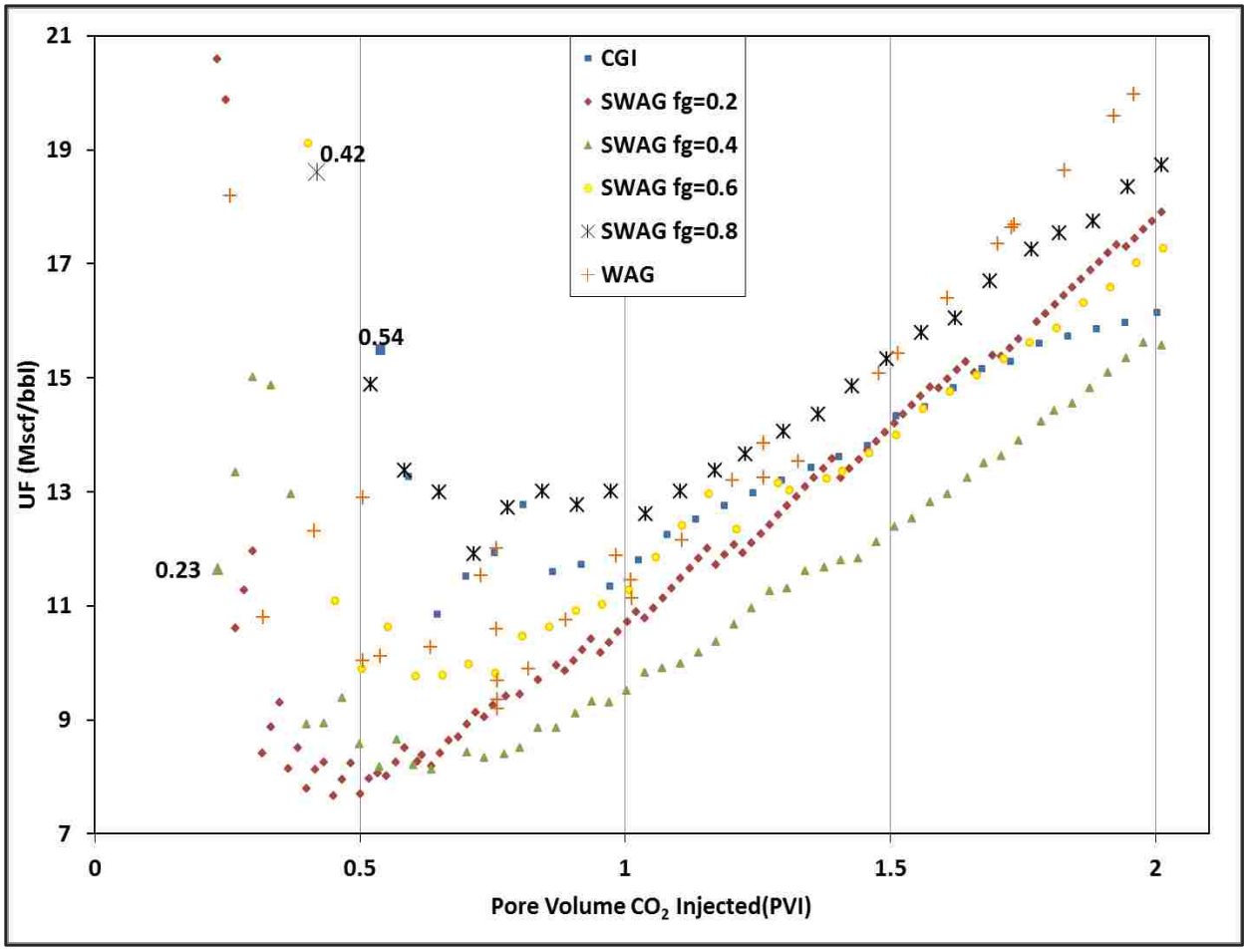

Figure 17: Comparison of Utilization Factor over 2 Pore Volumes of CO_2 Injected

Until about 1.3 pore volumes of CO_2 was injected, the gas utilization trends for SWAG with f_g = 0.2 and f_g = 0.4 outperform the other experiments. The gas utilization trend for SWAG

with f_g = 0.6 follows WAG until about 1.3 pore volumes of CO_2 have been injected. After about 0.5 pore volumes of injected CO_2 the SWAG with f_g = 0.4 maintained the lowest gas utilization factor followed by CGI. SWAG with f_g = 0.6 and 0.2 follows similar trend after about 1.4 pore volume of injected CO_2. Until about 0.5 pore volumes of CO_2 was injected, the SWAG floods with f_g = 0.2 and 0.4 followed almost similar paths. The SWAG flood with f_g = 0.2 reaches the lowest value of all the experiments. After 0.5 PV of CO_2 injected, the SWAG with f_g = 0.2 had a steep slope while SWAG at f_g = 0.4 maintained a much lower gas utilization factor. The CGI flood outperforms the SWAG at f_g = 0.6 towards the end when it experiences a bit more oil production.

When about one pore volume of CO_2 was injected, SWAG at f_g = 0.4 had the lowest gas utilization followed by SWAG at f_g = 0.2 and 0.6, followed by WAG and CGI floods. Similarly while scanning along the 1.5 pore volumes of CO_2 injected, SWAG at f_g = 0.4 outperformed all other floods followed by SWAG at f_g = 0.2 and 0.6 and CGI The graph of gas utilization versus pore volumes of total injection is shown in Figure 19 in Appendix B.

3.4 Summary:

The recoveries from CGI and WAG are characterized by an initial sharp shock producing significant amount of mobilized oil. The recoveries at late time are more likely due to rarefactions. During the CGI flood, water recovery at breakthrough was significant with very little production after the shock. However in the WAG flood the water saturation fluctuated.in response to the water and gas slug being injected In the SWAG floods the oil recoveries were likely due to long rarefaction rather than a sharp shock. However the oil recoveries matched or outperformed the CGI flood at early times (until 1.3 PVI) except SWAG at f_g = 0.8. SWAG floods. The effective viscosity increased with increase in fractional flow of gas until f_g= 0.4. Any further increase in f_g value decreased the effective viscosity. This behavior was analogous to the

two flow regime concept observed during N_2 foam flow through porous media. The water recoveries during the SWAG floods were dependent on f_g as higher gas fractional flows produced higher the water recovery factors. The SWAG with the lowest f_g value had the highest end point water saturation. The SWAG process at f_g= 0.4 recovered most of the residual oil even in the presence of relatively high water saturations. This was most likely due to highest effective viscosity achieved during this flood compared to all other floods. The gas utilization of SWAG floods equaled or outperformed the WAG and CGI floods until about 1.5 pore volumes of CO_2 was injected with the exception of SWAG with f_g=0.8.

The recoveries from the CGI injection process are good if the CO_2 contacts the oil. However heterogeneities in the formation and low viscosity of CO_2 results in poor sweep and hence require mobility control. Mobility control through WAG is useful but it can shield the residual oil from contacting the CO_2 .However SWAG must be designed properly to obtain optimum f_g value for obtaining higher effective viscosity and higher CO_2-oil contact.

4 CONCLUSIONS AND RECOMMENDATIONS

This work has dealt with evaluation of simultaneous water and gas injection in comparison to the conventional continuous gas injection and water alternating gas injection processes all using CO_2, to characterize the tertiary displacement during each experiment. In addition the intention was also to test the dependence of oil recovery in the SWAG process on the f_g values. The work in this thesis began with building a high pressure core flooding apparatus compatible to CO_2. Results from primary imbibition, primary drainage (oil flood) and secondary drainage (waterflood) process where discussed. The absolute permeability (k), end point oil and water permeabilities (k_{ro}° and k_{rw}°), connate water saturation (S_{wc}) and residual oil saturation after water flood ($(S_{or})_{wf}$) were determined to have reasonable confidence in the consistency between experiments. This work was able to consistently clean the core to a near native state, rather than using new and expensive cores for each experiment to make meaningful comparisons.

To understand the flooding performance of the tertiary recovery process the results were analyzed and discussed in Sections 3.2.3 and 3.3. To understand the results residual oil recovery, tertiary recovery factor and gas utilization were used. Based on the results from this study the following observations were made. These observations will lead to the important conclusions of this study followed by recommendations for future work.

1. The SWAG process with f_g= 0.4 recovered most of the residual oil even a at relatively higher water saturation. Continuous gas injection recovered the second-most. The recoveries from the WAG and the SWAG with f_g= 0.6 are similar but higher than the remaining SWAG floods.
2. All of the SWAG floods except the one at f_g= 0.8 outperformed the CGI process in recovering oil until about one pore volume of CO_2 injected. The CGI flood outperformed the WAG and the SWAG with f_g= 0.6 only after about 1.8 and 1.9 pore

volume of CO_2 injected. The SWAG floods with the exception of f_g= 0.8 closely matched the WAG oil recoveries until about 0.7 pore volume of CO_2 injected.

3. The SWAG flood with f_g= 0.2 and 0.4 had similar gas utilization factor values below 0.5 pore volume of CO_2 injected; in this region the SWAG with f_g= 0.2 reaches the lowest gas utilization value. At the same time the WAG and the SWAG flood with f_g= 0.6 had similar intermediate utilization values followed by the CGI and the SWAG flood at f_g= 0.8. At about one pore volume of CO_2 injected the SWAG with f_g= 0.6 had the lowest utilization. The CGI process outperformed the SWAG with f_g= 0.2 and 0.6 only towards the end.
4. In the SWAG process using CO_2 the pressure drop responses were similar to those described by two flow regime concepts for N_2-foam flow through porous media. This most likely indicates dispersed flow of CO_2 and water
5. The absolute permeability (k) values of the core were regained with reasonable consistency with the exception of experiments 1 and 2 when isopropyl alcohol was used instead of methanol. The connate water saturation (S_{wc}), end point oil and water permeabilities (k_{ro}° and k_{rw}°), and residual oil saturation after waterflood ($(S_{or})_{wf}$) values were closely regained throughout the study.

Based on these observations the following conclusions can be made:

I. In the SWAG process using CO_2, tertiary oil recovery has definite dependence on the gas fractional flow values.

II. The SWAG process using CO_2 appears to have recovery performance that is as good and in some of the cases presented better performance than the CGI and the WAG floods. This appears to be because of the higher effective viscosities which help to contact residual oil in the smaller pores. However this process must be designed to

operate at an optimum gas fractional flow value. During the WAG floods larger water slugs may shield the residual oil while the CGI flood most likely may not contact the oil trapped in low permeability zones.

III. The CGI and the WAG process recovered the most of their oil by a sharp shock wave presumably by building an oil bank, while the recoveries from the SWAG process were by mostly long rarefactions.

IV. All the SWAG floods except the one with f_g= 0.8 had better gas utilization until about 1.3 pore volumes of CO_2 injected. One pore volume or higher CO_2 injection amounts are large values which are only occasionally attained during field-scale CO_2 injection processes.

V. The core exposed to n-decane was cleaned to reasonably regain the native state. This was important to make meaningful comparisons without using the expensive new core for each experiment.

Based on the observation from this study, recommendations for future work include performing the SWAG floods with visual aid to test the dispersion of gas in water. Testing the SWAG process without a filter and comparing the performance with the results from this study is also recommended. In addition it would be a good idea to include the f_g values of 0.1, 0.3. 0.5, 0.7 and 0.9 in future SWAG studied with CO_2.

REFERENCES

Aleidan, A., and Mamora, D.D., 2010. $SWACO_2$ and $WACO_2$ Efficiency Improvement in Carbonate Cores by Lowering Water Salinity. Paper CSUG/SPE-137548 in the proceedings of Canadian Unconventional Resources & International Conference, Calgary, Alberta, Canada, 19-21October.

Alvarez, J.M., Rivas, H.J. and Rossen, W.R., 2001. Unified Model for Steady-State Foam Behavior at High and Low Foam Qualities. *SPE Journal*, **6**(3): 325-333. SPE-74171.

Amyx, J.W., Bass, D.M. and Whiting, R.L., 1960. *Petroleum Reservoir Engineering*. Mcgraw-Hill Book Company, 133-210 pp.

Anderson, W.G., 1986. Wettability Literature Survey- Part 1: Rock/Oil/Brine Interactions and the Effects of Core Handling on Wettability. *SPE Journal of Petroleum Technology*, **38**(10): 1125-1144. SPE-13932-PA.

Attanucci, V., Aslesen, K.S., Hejl, K.A. and Wright, C.A., 1993. WAG Process Optimization in the Rangely CO2 Miscible Flood. Paper SPE-26622 in the proceedings of SPE Annual Technical Conference and Exhibition, Houston, Texas, 3-6 October.

Ayirala, S.C. and Rao, D.N., 2006. Comparative Evaluation of a New MMP Determination Technique. Paper SPE-99606 in the proceedings of SPE/DOE Symposium on Improved Oil Recovery, Tulsa, Oklahoma, USA,22-26 April.

Azari, M., and Leimkuhler, J.M., 1990. Formation Permeability Damage Induced by Completion Brines *Journal of Petroleum Technology*, **42**(4):486-492.SPE-17149-PA.

Berge, L.I., Stensen, J. A., Crapez, B. and Quale, E.A., 2002. SWAG Injectivity Behavior Based on Siri Field Data. Paper SPE-75126 in the proceedings of SPE/DOE Improved Oil Recovery Symposium, Tulsa, Oklahoma, USA, 13-17 April.

Bortkevich, S.V., Kostrov, S.A., Savitsky, N.V. and Wooden, W.O., 2005. Method and Apparatus For Enhanced Oil Recovery by Micro-Dispersed Gas-Liquid Mixture into Oil Bearing Formation. US Patent. No. 2005/0077636A1.

Caudle, B.H. and Dyes, A.B., 1958. Improving Miscible Displacement by Gas-Water Injection. SPE-911-G. *Trans*., AIME **213**: 281-284.

Chang, S.-H. and Grigg, R.B., 1994. Effects of Foam Quality and Flow Rate on CO_2-Foam Behavior at Reservoir Temperature and Pressure. *SPE Reservoir Eval. & Eng.* **2**(3): 248-254. SPE-56856-PA.

Craig, F.F., 1971. *The Reservoir Engineering Aspects of Waterflooding*. Monograph Series. SPE, Richardson,TX.

Elsharkawy, A.M., Poettmann, F.H. and Christiansen, R.L., 1992. Measuring Minimum Miscibility Pressure: Slim-Tube or Rising-Bubble Method? Paper SPE-24114 in the proceedings of SPE/DOE Enhanced Oil Recovery Symposium, Tulsa, Oklahoma, USA, 22-24 April.

Enick, R., M., Beckman, E.,J., Shi, C.,Huang , Z., Xu , J., and Kilic , S., 2000. Direct Thickeners for Carbon Dioxide. Paper SPE-59325 in the proceedings of SPE/DOE Improved Oil Recovery Symposium, Tulsa, Oklahoma, USA, 3-5 April..

Enick, R.M. and Klara, S.M., 1992. Effects Of CO_2 Solubility in Brine on the Compositional Simulation Of CO2 Floods. *SPE Reservoir Engineering*, **7**(2):253-258.

Espinoza, D.A., Caldelas, F.M., Johnston, K.P., Bryant, S.L. and Huh, C., 2010. Nanoparticle-Stabilized Supercritical CO_2 Foams for Potential Mobility Control Applications. Paper SPE-129925 in the proceedings of SPE Improved Oil Recovery Symposium, Tulsa, Oklahoma, USA, 24-28 April.

Fu, B., McMahon, A., J. and Blakley, K., 1998. The Controversy of CO_2 Solubility in Water, in the proceedings of CORROSION 98. NACE International, San Diego California.

Gabriel, G.A. and Inamdar, G.R., 1983. An Experimental Investigation of Fines Migration in Porous Media. Paper SPE-12168 in the proceedings of SPE Annual Technical Conference and Exhibition, San Francisco, California, 5-8 October.

Garcia, J., E., 2001. Density of Aqueous Solutions of Carbon dioxide, Lawrence Berkley National Laboratory, 10 October 2001. http://escholarship.org/uc/item/6dn022hb.

Glass, O., 1985. Generalized Minimum Miscibility Pressure Correlation. *SPE Journal*. **25**(6): 927-934. SPE-12893-PA.

Green, D.N. and Willhite, P.G., 1998. *Enhanced Oil Recovery*. Society of Petroleum Engineers, **6**.

Heller, J., Dandge, D., Card, R. and Donaruna, L., 1985. Direct Thickeners for Mobility Control of CO_2 Floods. *SPE Journal*: **25**(5):679-686. SPE-11789-PA.

Jarell, P.M., Fox, C.E., Stein, M.H. and Webb, S.L., 2002. *Practical Aspects of Carbon-Dioxide Flooding.* Monograph Series, SPE, Richardson, Texas, USA.

Kia, S.F., Fogler, H.S. and Reed, M.G., 1987. Effect of Salt Composition on Clay Release in Berea Sandstones. Paper SPE-16254 in the proceedings of International Symposium of Oilfield Chemistry, San Antonio, Texas, USA, 4-5 February.

Klins, M.A., 1984. *Carbon Dioxide Flooding*, Chap. 3, 105-137, International Human Resources Development Corporation, Boston.

Kulkarni, M.M., 2003. Immiscible and Miscible Gas-Oil Displacement in Porous Media. MS Thesis, Louisiana State University, Baton Rouge. LA, USA.

Kulkarni, M.M. and Rao, D.N., 2004. Experimental Investigation of Various Methods of Tertiary Gas Injection. Paper SPE-90589 in the proceedings of SPE Annual Technical Conference and Exhibition, Houston, Texas, USA, 26-29 September.

Lake, L., 1989. *Enhanced Oil Recovery*. Prentice Hall Professional Technical Reference

Ma, T.D., Rugen, J.A., Stoisits, R.F. and Youngren, G.K., 1995. Simultaneous Water and Gas Injection Pilot at the Kuparuk River Field, Reservoir Impact. Paper SPE- 30726 in the proceedings of SPE Annual Technical Conference and Exhibition, Dallas, Texas, USA, 22-25 October.

McCain Jr., W.D., 1990. *The Properties of Petroleum Fluids*. PennWell Publishing Company, Tulsa, Oklahoma, USA.

Moritis, G., 2010 Worldwide EOR Survey. *Oil and Gas Journal*, **108**(14).

National Institute of Standards and Technology, 2008. *Isothermal Properties of Carbon dioxide*., http://webbook.nist.gov/cgi/fluid.cgi?T=24&PLow=0&PHigh=2500&PInc=50&Applet=on&Digits=5&ID=C124389&Action=Load&Type=IsoTherm&TUnit=C&PUnit=psia&DUnit=g%2Fml&HUnit=Btu%2Flb-mole&WUnit=ft%2Fs&VisUnit=cP&STUnit=dyn%2Fcm&RefState=DEF (accessed 03 February 2010)

National Institute of Standards and Technology, 2008. *Isothermal Properties of Normal Decane*. http://webbook.nist.gov/cgi/fluid.cgi?T=24&PLow=0&PHigh=2500&PInc=50&Applet=on&Digits=5&ID=C124185&Action=Load&Type=IsoTherm&TUnit=C&PUnit=psia&DUnit=g%2Fml&HUnit=Btu%2Flb-mole&WUnit=ft%2Fs&VisUnit=cP&STUnit=dyn%2Fcm&RefState=DEF (accessed 03 February 2010).

Osterloh, W.T. and Jante, Jr., M.J., 1992. Effects of Gas and Liquid Velocity on Steady-State Foam Flow at High Temperature. Paper-24179 in the proceedings of SPE/DOE Enhanced Oil Recovery Symposium, Tulsa, Oklahoma, USA, 22-24 April.

Parkinson, W., J., and de Nevers, N., 1969. Partial Molar Volume of Carbon Dioxide in Water solutions. *Journal of Industrial & Engineering Chemistry* **8**(4):709-713.

Persoff, P. and Pruess, K., 1995. Two-phase Flow Visualization and Relative Permeability Measurement in Natural Rough Walled Rock Fractures. *Water Resources Research*, **31**(5): 1175-1186.

Quale, E.A., Crapez, B., Stensen, J.A. and Berge, L.I., 2000. SWAG Injection on the Siri Field - An Optimized Injection System for Less Cost. Paper SPE-65165 in the proceedings of SPE European Petroleum Conference, Paris, France, 24-25 October.

Rao, D.N., 1997. A New Technique of Vanishing Interfacial Tension for Miscibility Determination. *Fluid Phase Equilibria*, **139**(1-2): 311-324.

Rao, D.N., Ayirala, S.C., Abe, A.A. and Xu, W., 2006. Impact of Low-Cost Dilute Surfactants on Wettability and Relative Permeability. Paper SPE-99609 in the proceedings of SPE/DOE Symposium on Improved Oil Recovery, Tulsa, Oklahoma, USA, 22-26 April.

Rapoport, L.A. and Leas, W.J., 1953. Properties of Linear Waterfloods. SPE 213-G. *Trans*., AIME **198**: 139-148

Reamer, H.H. and Sage, B.H., 1963. Phase Equilibria in Hydrocarbon System. Volumetric and Phase Behavior of n-Decane-CO_2 System. *Journal of Chemical &Engineering Data*, **8**(4): 508-513.

Robie, J., D.R., Roedell, J.W. and Wackowski, R.K., 1995. Field Trial of Simultaneous Injection of CO_2 and Water, Rangely Weber Sand Unit, Colorado. Paper SPE-29521 in the proceedings of SPE Production Operations Symposium, Oklahoma City, Oklahoma, USA, 2-4 April.

Sharma, M.M. and Filoco, P.R., 2000. Effect of Brine Salinity and Crude-Oil Properties on Oil Recovery and Residual Saturations. *SPE Journal*, **5**(3): 293-300.SPE-65402-PA.

Sohrabi, M., Danesh, A., and Jamiolahmady, M., 2008 Visualization of Residual Oil Recovery by Near-miscble Gas and SWAG Injection Using High-Pressure Micromodels. *Transport in Porous Media*,**74**: 239-257

Shaw, J.C., Churcher, P.L. and Hawkins, B.F., 1991. The Effect of Firing on Berea Sandstone. *SPE Formation Evaluation*, **6**(1): 72-78.SPE-18463-PA.

Stephenson, D.J., Graham, A.G. and Luhning, R.W., 1993. Mobility Control Experience in the Joffre Viking Miscible CO2 Flood. *SPE Reservoir Engineering*, **8**(3): 183-188. SPE-23598-PA.

Stoisits, R.F., Krist, G.J., Ma, T.D., Rugen, J.A., Kolpak, M.M., and Payne, R.L., 1995. Simultaneous Water and Gas Injection Pilot at the Kuparuk River Field, Surface Line Impact. Paper SPE-30645 in the proceedings of SPE Annual Technical Conference and Exhibition, Dallas, Texas, USA, 22-25 October.

Tiffin, D.L, and Yellig, W.F., 1983. Effects of Mobile Water on Multiple-Contact Miscible Gas Displacements. *SPE Journal* **23**(3):447-455. SPE-10687-PA.

APPENDIX A: REVIEW OF SWAG STUDIES

This section will discuss in greater detail a few of the relevant laboratory studies on simultaneous water and gas injection mostly using CO_2. The intention here was to understand the experimental setup and procedures to interpret the presented results. Some of the relevant studies that are discussed in this section are:

Caudle and Dyes (1958)

Caudle and Dyes (1958) used a five-spot square micromodel for their experiments. The micromodel was 10 inches wide and 0.25 inch thick. It had four injecting wells at the corners and a producer at the center. The objective of the study was to evaluate sweep efficiency of the miscible gas injection processes. Four recovery experiments were performed namely: waterflood, miscible gas drive, immiscible gas drive (low pressure) and simultaneous injection of gas and water. The miscible simultaneous injection process was carried out with 0.3 pore volumes of gas ahead of simultaneous water and gas injection at a gas fractional flow value of 0.7.

The results were plotted as the percentage of oil recovered versus pore volumes injected. The breakthrough of the injected fluid was quickest for immiscible gas flood when 0.25 pore volumes had been injected, followed by miscible gas injection and waterflood at about 0.4 pore volumes injected. The gas breakthrough for SWAG injection was when 0.6 pore volumes had been injected. Highest sweep efficiency of about 90% was achieved by SWAG injection followed by waterflood and miscible gas drives of about 60%. The lowest sweep efficiency was observed during immiscible gas injection.

Tiffin and Yellig (1983)

Tiffin and Yellig (1983) studied the effect of mobile water saturation on multiple contact miscible displacements. They used Berea sandstone cores in their experiments and all cores were

8 feet long and 2 inches in diameter. The core was wrapped with epoxy and fiberglass tapes. All the floods were carried out at a back pressure of 1900 psia and 130 ^{o}F, with an annulus pressure of 2000 psi. Constant rate Ruska pumps were used to inject the fluids from the transfer vessels. A back pressure regulator was used in the CO_2 line and a check valve was used in the water line before a T-section where the two lines converged. The produced fluids were passed through a sight glass under the test conditions. The fluids were then flashed to atmosphere. The gas production was recorded by a wet test meter and analyzed by a gas chromatograph. The separator liquids were collected and analyzed for composition using the gas chromatograph.

The separator gas and oil were analytically recombined at the end of each experiment using GOR, phase composition and liquid and gas densities. The recombined compositions were subdivided into CO_2, C_1, C_2 through C_6 and C_{7+} fractions. These fractions were normalized by the amount of each fraction in the original reservoir oil.

Two sets of experiments were performed using Berea sandstone core, one in a water wet state and the other in an oil wet state. The average permeability of water wet cores was 365.5 mD and that of oil wet cores was 187 mD. The oil was recombined reservoir oil with viscosity of 0.35 cP and bubble point pressure of 1660 psi. The brine was 0.25 N NaCl solution with viscosity of 0.51 cP at 130 ^{o}F. The minimum miscibility pressure for this CO_2/oil system was estimated to be 1660 psi based on series of slim tube tests at 130 ^{o}F.

The density and viscosity of the CO_2 under the experimental conditions were 0.598 g/cc and 0.052 cP. All the waterfloods and continuous gas injection processes and some SWAG floods were performed at total injection rate of 0.117 cc/min. A secondary gas injection, a tertiary gas injection and three tertiary simultaneous water and gas injection processes, were conducted using CO_2 under water wet state. Here SWAG injection was carried out at two different f_g values of 0.57 and 0.76. The SWAG flood at f_g = 0.57, was performed at two different

total injection rates of 0.117 cc/min and 0.065 cc/min. A tertiary continuous gas injection and three tertiary SWAG floods were performed using CO_2 in oil wet state. Here the SWAG floods were performed at f_g values 0.57 and 0.24.

In water wet cores waterflood oil recovery ranged from 40.1% to 41.9% of OOIP. The continuous gas injection process recovered 89.4% OOIP and 82.3% of residual oil left after waterflooding. A SWAG injection process at f_g = 0.57 recovered 47.5% and 63.9% of residual oil left after waterflood corresponding to total injection rate of 0.117 cc/min and 0.065 cc/min respectively. The SWAG process at f_g value of 0.76 also recovered almost the same fraction of residual oil. Therefore it is likely that at lower injection rates CO_2 had more time to diffuse through the water and produce the water-shielded oil. In the oil wet case the waterflood recovery ranged from 55% to 60.2% of the OOIP. CGI in oil wet cores recovered about 95.5% of OOIP and 90% of residual oil left after waterflood. The SWAG process at total injection rate of 0.117 cc/min with fractional flow of gas values of 0.57 and 0.24 recovered 82.5% and 72.5% of residual oil left after waterflood. It was observed from the results that oil recoveries during SWAG injection process showed dependence on f_g value and the total injection rates both in water wet and oil wet cores. Higher recoveries during miscible SWAG were observed and were most likely due to higher fractional flow value of gas and lower injection rate. At lower total injection rates CO_2 had higher time to diffuse in order to contact the water shielded oil. Oil recoveries from oil wet cores are higher than that in water wet cores.

Stoisits et al (1995)

Stoisits et al (1995) presents the results of laboratory studies to address phase separation at the joints during simultaneous water and gas injection along with the results of pilot tests at Kapurak River field in Alaska.

The laboratory experiments involved investigating phase splitting during simultaneous injection of water and air. The following configurations were tested: branching tee, branching tee with surfactant injection, branching tee with static mixers and branching tee with static mixers and mechanical splitter. SWAG injection with static mixers and surfactant injection significantly reduced the phase splitting. However it was concluded that SWAG injection with static mixers was the most favorable for field scale implementation. From the laboratory study it was concluded that at the superficial velocity values approaching the horizontal, the upward and the downward branches should be about 6-7 feet/sec, 7-8 feet/sec and 5-6 feet/sec respectively to prevent phase-splitting.

Based on these results pilot tests for the SWAG processes were conducted at the Kapurak River field. The pilot configuration had capabilities to inject gas into the diffuser of the water injection line. The gas and liquid from the diffuser flowing through the static mixer were supplied to two well sites. One of the two drill sites was located along the horizontal branch (Drill Site 2D) of the main tee while the other was on the vertical branch (Drill Site 2E). The site 2D was further divided using another tee into left and right branches. Each branch had four wells. All the wells in each branch had static mixtures at their well head except the last wells. Site 2E had three wells without static mixers. Pilot tests numbered 1-6 were performed for 17 days with the gas-liquid ratios values (scf of gas per barrel of produced water) at the diffuser site ranging from 55 scf/bbl to 181 scf/bbl. Site 2E was tested only at a gas-liquid ratio of 55 scf/bbl as the wells shut in sequentially from the bottom to top due to gas holdup. Site 2D was tested at GLR values of 55 scf/bbl, 70 scf/bbl, 100 scf/bbl, 143 scf/bbl, 121 scf/bbl and 181 scf/bbl. During the test with GLR value of 121 scf/bbl (test number 5) and 181 scf/bbl (test number 6), the right hand branch of site 2D was utilized while the left was shut-in.

The results from each test were presented as a table with details about the well, volumetric rates, velocity in the main run, velocity in the side branches and liquid fractions. Based on results from test 2-4 it was observed that even with velocity values in the side arm lower than critical velocity, phase splitting was not observed as the velocities in the main run was more than the critical value. The velocity in the main run was considered more vital compared to that in side arm

During test 5, with main run velocity higher and side arm velocity lower than the laboratory scale critical velocity the gas was observed only in the first well (well 2D-16). In test number 6, the gas was observed only in the first well (well 2D-16) even when main and side arm velocities were lower than laboratory scale critical velocity. This indicates that the efficiency of static mixtures depends not only on the main run velocity but also on the gas to liquid ratio. A table of measured and calculated bottom-hole pressures for well 2D-16 for various gas-liquid ratios were presented. The bottom hole pressures were calculated using the Beggs and Brill correlation and the no slip (between gas and liquid) pressure drop calculation. The measured pressure closely agreed to the no-slip pressure drop calculation.

The results from the study indicate that phase separation of water and gas depends on the fractional flow value of gas, critical flow velocities for a given static mixer. In addition the bottom-hole pressure calculated based on no-slip condition agreed better to the observed bottom-hole pressures compared to the Beggs and Brill calculation at all gas to liquid ratio value except at 121 scf/bbl suggesting a dispersed air in water type flow during SWAG process.

Chang and Grigg (1999)

Chang and Grigg (1999) designed experiments to study the effect of foam quality and injection rates on CO_2 foam mobility. They used four fired Berea sandstone cores in their experiments. The cores were labeled A, B, C and D with measured initial brine permeability of

about 37 mD, 196 mD, 139 mD and 62 mD respectively. All of the cores were 1.27 cm in diameter. Core A had a length of 5.21 cm, core B was 6.25 cm long, core C was 2.52 cm long and core D was 1.24 cm long.

Three accumulators were used, one to inject brine, second one to inject surfactant solution and the third one to inject CO_2 into the core. Separate pumps were used to pump water to the bottom of the accumulator to inject CO_2 and brine or surfactant solution from the top. The system pressure was maintained at 2100 psig by the back pressure regulator connected near the outlet. The pressure drop across the core was recorded using a pair of pressure transducers and the differential pressure transducer. Gas production was monitored using the wet test meter. A surfactant solution was prepared using brine and Chevron CD chaser 1045 with a surfactant concentration of 2500 ppm. Oil was not used in these experiments. The brine composition was 3% NaCl, 0.03% KCl, 0.5% $CaCl_2$, 0.2% $MgCl_2$ and 0.3% Na_2SO_4.

Baseline experiments were performed by simultaneous injection of brine and CO_2 into the brine saturated core. The cores A, B and C were used during simultaneous water and CO_2 injection at different total injection rates of 8.4 cc/h, 4.2 cc/h and 16.8 cc/h. At each rate the gas fractional flow of 0.2, 0.333, 0.5, 0.667 and 0.8 were used. The injection continued until steady state pressure drop was attained.

The mobility of SWAG and foam was calculated assuming both as single phase fluids. CO_2 foam experiments were performed by simultaneous injection of surfactant solution and CO_2 into cores B, C and D. Cores B and D were used at total injection rates of 4.2 cc/h while core C was used at 4.2 cc/h, 8.4 cc/h and 16.8 cc/h. At each rate foam quality values of 20%, 33.3%, 50%, 66.7 and 80% were used.

The results of simultaneous water and CO_2 injection process were presented as a table and a graph of mobility versus fractional flow of gas. The table summarized all the simultaneous water and CO_2 injection experiments with values for total injection rates, fractional flow of gas (f_g), steady state pressure drop, total mobility and total interstitial velocity.

For the core A the total mobility value increased with increase in fractional flow of gas value from 0.33 to 0.8 and the mobility values increased with decrease in fractional flow of gas values less than 0.33. This behavior was consistent at all injection rates. For core B and C, at injection rate of 16.8 cc/h the total mobility values increased with increase fractional flow of gas values from 0.33 to 0.8. The total mobility increased by decreasing the fractional flow of gas values less than 0.333. But at all other rates the mobility value increased with increase in fractional flow of gas value from 0.2 to 0.8.

During the foam experiment with foam quality of 33.3%, a graph of pressure drop versus foam quality showed a differential pressure cycling with amplitude of 70-80 psi. The differential pressure cycling for foam quality of 50% reduced to about 50-60 psi. While the differential pressure cycling almost disappeared at foam qualities of 66.7% and 80%. The researchers also observed the smaller pressure cycling in simultaneous water and CO_2 injection.

Based on the results observed during SWAG process, the value of fractional flow of gas at which the pressure response shifts depends on the core's permeability, fractional flow of gas and the total injection rate.

Bortkevitch et al (2005)

Bortkevich et al (2005) developed a process and apparatus to produce micro-dispersed gas liquid mixture. Two apparatus were developed to create micro-dispersed gas-liquid mixture. One

when gas pressure would be 0-20% less than the liquid pressure and another when gas pressure would be 0.1-20% higher than the liquid pressure.

In the case of higher gas pressures an apparatus was developed by sequential vertical assembly of a gas-liquid ejector unit, a cavitation unit and a jet dispersing unit. The communication between each unit was through the conical orifice. Water entered the device axially into a nozzle while gas was drawn in the direction perpendicular to water flow into the ejection chamber. Both water and gas were isolated from each other in the ejector chamber. The water stream from a nozzle mixed with gas flowing through an orifice in the cavitation chamber to form the first gas liquid mixture. The nozzle and orifice dimension were tuned to obtain desired fractional flow of gas and water. The cavitation unit comprised of a C-shaped chamber tangentially connected to a hollow cylindrical cavitation unit. The first gas-liquid mixture was rotated in the cavitation unit that reportedly developed an unstable cavity along the axis of symmetry which collapses generating micro-shocks. The micro-shocks broke and further homogenized the first gas-liquid mixture. The homogenous gas liquid mixture was then introduced into the jet-dispersing chamber through the second nozzle. The flow was then made to dip down and impinge on to a bottom plate reportedly producing a pulsating cavity which created micro dispersed gas-liquid mixture. The micro dispersed gas-liquid mixture then moved to the outlet of the unit into the jet dispersing chamber. The chamber was C-shaped connected to the outlet of the apparatus. In the case of lower gas pressure the apparatus was just vertical assembly of a cavitation unit and a jet dispersing unit. The gas was supplied radially into the C-shaped hollow cavitation chamber using an orifice and the liquid was supplied axially into the cavitation unit. The gas tangentially enters the cavitation unit and mixes with the incoming liquid. The first gas-liquid mixture was rotated to form finer gas-liquid mixture as mentioned above. The finer gas-liquid mixture was introduced into the jet-dispersing unit through a second

orifice. The flow was diverted to dip-down to impinge onto the bottom plate further breaking finer gas-liquid mixture to micro-dispersed gas-liquid mixture which communicated to the outlet of the device.

A field test of the apparatus was carried on an oil zone in the Samotlor oil field in West Siberia and reported the following values. The average pore size of the zone was 150 microns. The micro-dispersed gas-liquid mixture had bubble size of 30-40 micron. The gas content in the mixture was 10-40 percent. The formation was injected with micro-dispersed gas-liquid mixture for 12 months using 28 injection wells with cumulative gas injection of 18.4 million standard cubic meters. The apparatus was supplied with gas at pressure of about 1160-1900 psi which was 20 percent less than the liquid injection pressure. Prior to injection of micro-dispersed gas-liquid mixture the average injection rate was 500 tons/day per well to attain average production of 9.6 tons/day of oil per well with 96 percent water cut and 304 tons/day of fluid per well from 90 producing wells. The additional cumulative oil produced of 21000 tons.

Sohrabi et al (2008)

Sohrabi et al (2008) performed high pressure micromodel studies to visualize oil recovery by near miscible gas and SWAG injection. The micromodel had two glass plates: a bottom plate and a cover plate. Two dimensional pore structures of 6 mm wide and 38 mm long were etched on the bottom plate. The flat cover plate with an inlet and outlet port was secured on the bottom plate creating the desired pore space. The depth of the pores was ranged from 35 μm to 45 μm and width ranging from 35 μm to 300 μm. The movement and interaction of the fluids was observed using a magnifying camera. The movement of the camera was controlled by a computerized linear drive system which was capable of sweeping the pore structure sequentially or continuously for video recording. The micromodel was designed for pressures and temperatures up to 6000 psi and 100 ^{o}F. Two low rate pumps were used to inject and collect the

produced (retract) fluid. Pressure transducers were used to monitor the injection, inlet, outlet, retraction and overburden pressures. The critical pressure for n-decane/methane system was 5300 psia at 100 ^{o}F. Hence the experiments were performed at 5100 psia and 100 ^{o}F to attain near miscibility between methane and decane. The viscosities of gas, oil and water were 0.0378 cP, 0.1085 cP and 0.67 cP respectively. The interfacial tensions (IFT) between gas-oil, gas-water and oil-water were 0.08 μNm^{-1}, 41 μNm^{-1} and 42 μNm^{-1} respectively. The viscosities and interfacial tension (IFT) were measured at experimental conditions.

Three tertiary recovery experiments were conducted: near miscible methane and simultaneous water and methane injection with fractional flow of gas values of 0.5 and 0.2. For each experiment the micromodel underwent similar oil and waterflood. The micromodel was initially saturated with distilled water which was colored blue. The water was produced by injecting n-decane (colorless) at a capillary number of $1x10^{-7}$ until oil was produced. The water wet characteristics of the micromodel was inferred based on the curvature of the oil-water interface. The oil was displaced from the pore space by flooding water at capillary number of $1x10^{-7}$ until oil production ceased. The fluid movement was video recorded. During near miscible gas injection methane was injected at velocity of 6.41×10^{-3} mm/sec, equal to the injection velocity during the waterflood.

During near miscible simultaneous water and methane injection both fluids were injected by two separate pumps. Methane and water were observed to enter the micromodel as two separate and continuous phases. The total injection rate during simultaneous water and gas injection was the same as in the near miscible methane injection.

The results were reported as snapshots of one of the sections of the micromodel showing the fluid distribution. For each experiment the snapshots during tertiary recovery were presented at gas breakthrough and 1 hour after the gas breakthrough. In near miscible methane injection, at

breakthrough the gas flow was predominantly through a single channel. But after 1 hour of injection the path of gas flow was wider predominantly concentrated towards the left half of the micromodel. The main difference observed between the two snapshots was that the near miscible methane injection recovered the oil bypassed by the gas front. The behavior was similar in the other two experiments. However near miscible SWAG injection at f_g value of 0.2 shows more uniform sweep. During SWAG floods no slug or bubbly flow was visually observed. Instead water flow was along the pore body and gas flow through the center of the pores. Even though the pressure gradients during the SWAG floods a fraction of a psi pressure differential was reported with no fluctuation observed. This led them to conclude that mass transfer between oil and gas was minimal. Oil recovery by near miscible simultaneous water and methane injection was independent of fractional flow of gas values.

Aleidan and Mamora (2010)

Aleidan and Mamora (2010) studied the effects of lowering brine salinity on miscible flooding using CO_2. The study involved performing slimtube tests and core floods. Slimtube experiments were performed to determine the minimum miscibility pressure of CO_2 in dead West Texas oil. The minimum miscibility pressure of 1800 psi was determined from slimtube tests based on benchmark recovery of 90% after 1.2 pore volumes of CO_2 have been injected.

All the corefloods were performed using a 2 inch diameter by 6 inches long limestone core with no clay content. The core had an average permeability value of 90 mD and a porosity of 29%. It was installed in a Nitrile® sleeve and secured using end plugs and end caps. A confining pressure of 2300 psi was applied to the core. The core holder was placed in an oven at set value of 120 ^oF. The injection system employed two positive displacement pumps and two transfer vessels. One pump injected brine directly into the core holder. The second pump injected distilled water into the bottom-end of a transfer vessel with oil or CO_2 on top. All the coreflood

experiments were performed with back pressure of 1900 psi. The backpressure regulator installed at the outlet of the core holder was operated using nitrogen gas.

The produced fluids were collected in the separator. The produced liquids were measured using a graduated cylinder while the produced gas was measured using a wet test meter. Two pressure transducers and thermocouples were used to monitor inlet and outlet pressures and temperatures. The pressure, temperature and wet test meter data were logged and recorded into a computer.

Four different types of secondary recovery experiments were performed in secondary recovery mode namely continuous gas injection, waterflood, water alternating gas and simultaneous water and gas injection, all using CO_2. Initially the core was saturated with NaCl brine followed by the measurement for permeability and porosity. The brine was displaced from the core by injecting West Texas oil to attain connate water saturation.

First the continuous gas injection (CGI) experiment was conducted by injecting CO_2 at a rate of 0.5 cc/min. Next waterflood experiments were conducted at brine salinity values of 0 and 6 weight percent followed by 1: 1 WAG experiments which were conducted at an injection rate of 0.5 cc/min and slug size of 0.333 pore volumes. Finally simultaneous water and gas experiments were conducted at a total injection rate of 0.5 cc/min with fractional flow of gas value of 0.5. WAG and SWAG experiments were performed at brine salinity values of 0, 6 and 20 weight percent. All the experimental results were presented as graphs of secondary recovery factor and pressure and pressure drop versus pore volumes injected. Gas injection processes had additional graphs of cumulative water and gas produced versus pore volumes injected. CGI recovered about 75% of the OOIP after about 1.7 pore volumes of CO_2 had been injected. CO_2 breakthrough was at about 0.12 pore volumes injected with a corresponding pressure drop of 10 psi.

CGI recovered about 50% of the OOIP when about 0.5 pore volumes of CO_2 had been injected. The approximately steady state pressure drop across the core was about 7 psi with about 1-2 psi of maximum fluctuations. In both the waterflood experiments water breakthrough was when 0.25 pore volumes had been injected with similar ultimate recoveries of about 54% of OOIP after 1.4 pore of had been injected.

WAG experiments had the highest ultimate recovery of about 93% when the brine salinity value was 0 weight percent followed by about 87% when the brine salinity was 6 weight percent and WAG had the least recovery of about 75% when brine salinity was 20 weight percent. All WAG experiments were performed until about 1.6 pore volumes had been injected. During all the SWAG experiments, gas and water breakthrough occurred when about 0.12 and 0.5 pore volumes had been injected. Breakthrough time was observed to be independent of salinity. Ultimate oil recoveries were observed to be dependent on the brine salinity. The highest recovery of 98.7% was achieved with 0 weight percent salinity, followed by 90.7% recovery at 6 weight percent salinity and 81.5% recovery at 20 weight percent salinity. The gas and water production starts when the oil production begins to decline. The approximate steady state and linear gas an water production begins when oil production begins to decline. The slope and cumulative gas produced were highest at highest salinity during SWAG process whereas the other two followed similar trends and had almost similar end points of about 17.5 compared to 20.5 standard liters of CO_2. The consistent stepwise trends in gas production indicate the blocking and opening of the gas paths. The approximately steady state pressure drop was about 8 and 7 psi respectively during highest and least salinity respectively with maximum fluctuations of 3 psi. The pressure drop data indicates blocking and opening of gas flow path with a possibility of bubble like flow of SWAG at a fractional flow of gas value of 0.5.

APPENDIX B: TRF AND UF VERSUS TOTAL PV INJECTED

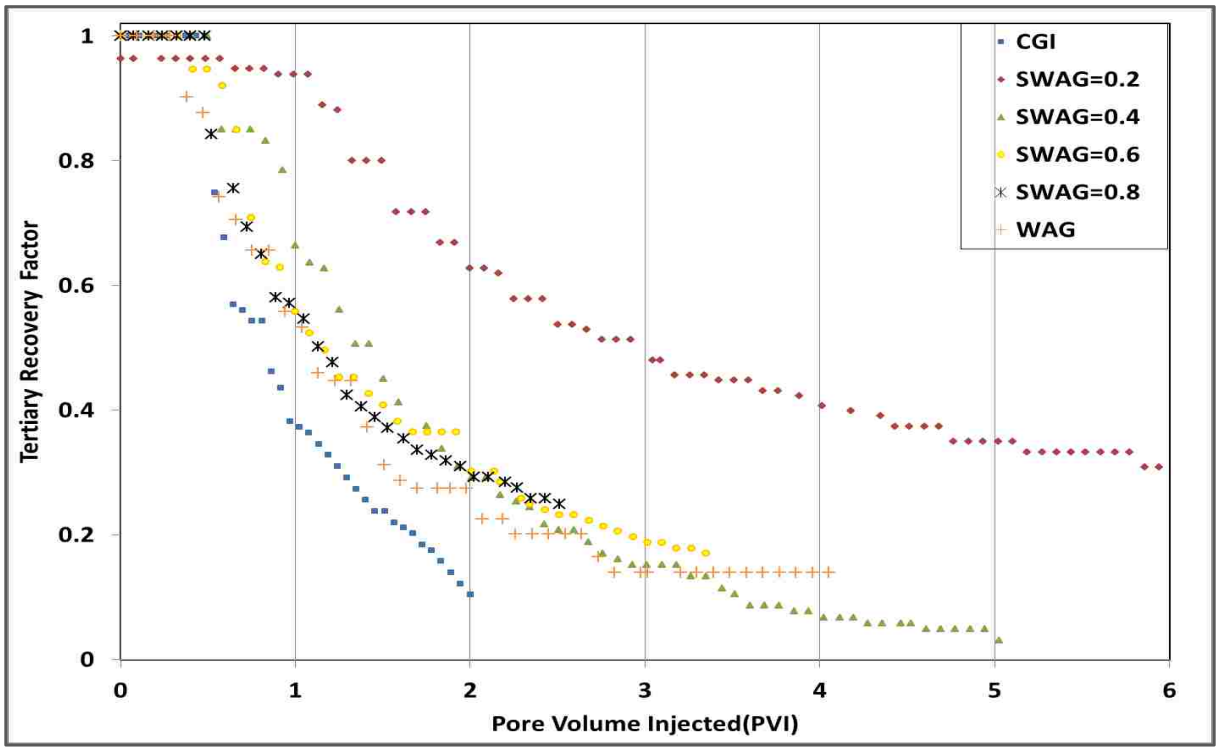

Figure 18: Comparison of Tertiary Recovery Factor over Total Pore Volumes Injected

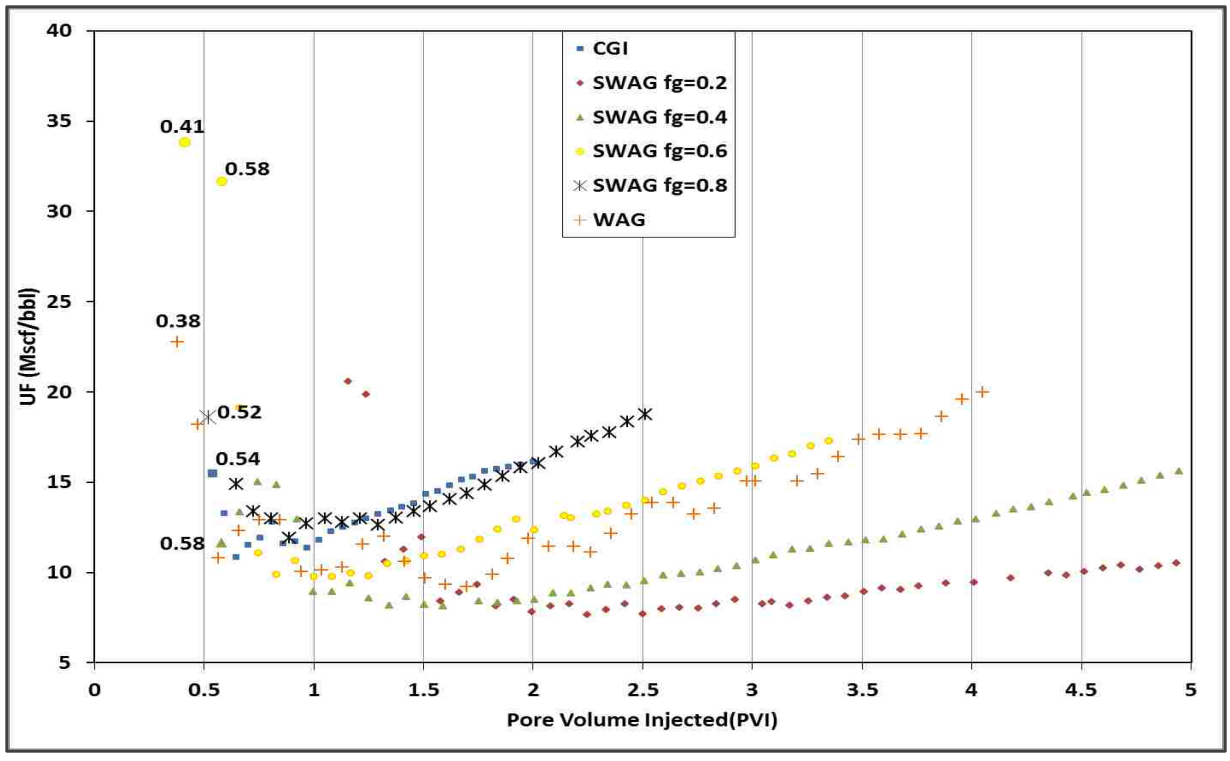

Figure 19: Comparison Utilization Factor over Total Pore Volumes Injected

APPENDIX C: LIST OF EQUIPMENT

Equipment	Specification	Vendor
ISCO 260 D Syringe Pump	Capacity: 266 ml Flow range: 0.001-107 ml/min. Pressure rating: 0-7500 psi.	Teledyne Isco, Inc. 4700 Superior Street Lincoln NE 68504 http://www.isco.com/
Pressure Tapped Core Holder	Hassler type Core diameter: 1 inch Core length: 12 inches. Pressure rating: 0-5000 psi Five pressure taps over 10 inches	Temco- CoreLab Instruments 4616 North Mingo Tulsa, OK 74117-5901. Phone: 918-834-2337. http://corelab.com/
Back Pressure Regulator	Tescom Air actuator Model: 26-1764-24-285A. Pressure range: 0-2500 psi, C_v: 0.2. Applied to control pressure: 1:30. Accuracy: 1% full scale.	John H. Carter, Co., Inc. 2728 N. Arnoult Road, Metairie, LA 70002 Phone: 505-887-8580. http://www.johnhcarter.com/
Berea Sandstone	Core diameter: 1 inch. Core length: 12 inches. Cut parallel to bedding plane.	Cleveland Quarries 850 West River Rd. Vermillion, Ohio 44089 Phone: 1800- 248-0250. http://www.clevelandquarries.com/
Fluid Transfer Accumulator	Piston Type Capacity: 1000 cc. Pressure rating: 0-5000 psi.	Temco- CoreLab Instruments 4616 North Mingo Tulsa, OK 74117-5901. Phone: 918-834-2337. http://corelab.com/
Tube and Tube Fittings	Swagelok Company	Capital Valve & Fittings Co. 9243 Interline Ave, Baton Rouge LA 70809 Phone: 225-926-5520 http://www.swagelok.com/
Pressure Transducers	Model# PX 309-5KGV5V. Pressure: 0-5000 psi. Power supply: 0-5 V DC. Output signal: 0-5 V. Accuracy: 0.25% full scale.	Omega Engineering, Inc. One Omega Drive P.O. Box: 4047 Stamford CT 06907 Phone: 1800-848-4286 http://www.omega.com/
Digital Transmitter	Omega DIN-113. Signal to RS 485 converter. Power supply: 0-5 V DC. Input signal: 0-5 V. Output signal: RS-485. Accuracy: 0.02% full scale.	Omega Engineering, Inc. One Omega Drive P.O. Box: 4047 Stamford CT 06907 Phone: 1800-848-4286 http://www.omega.com/

Equipment	Specification	Vendor
Digital Converter/Repeater	Omega DIN-191 RS 232/ 485 converter Power supply: 0-5 V DC Input: RS-232/RS 485. Output: RS-485.	Omega Engineering, Inc. One Omega Drive P.O. Box: 4047 Stamford CT 06907 Phone: 1800-848-4286 http://www.omega.com/
Data Acquisition Module	Macro enabled MS-Excel® Spreadsheet Language: Visual Basic	Darryl Bourgoyne Director Well Facility Craft & Hawkins Dept. of Petroleum Engineering Louisiana State University. Phone: 225-578-8458 e-mail: dbourg1@lsu.edu
Three Way Valve	Catalog # 15-15AF2 Pressure: 0-15,000 psi. Two stem connection.	High Pressure Equipment Co. P.O. Box 8248, 1222 Linden Erie, PA 16505 Phone: 1800-289-7447
Inline Filter	Catalog # 15-51AF2 Size: 2 micron. Pressure: 0-15,000 psi.	High Pressure Equipment Co. P.O. Box 8248, 1222 Linden Erie, PA 16505 Phone: 1800-289-7447
Hydraulic Hand Pump	ENERPAC P-80 Capacity: 134 cubic inches Grainger item # 4Z481	Grainger Phone: 1800-323-0620 http://www.grainger.com/
Vacuum Pump	Welch Duoseal® Vacuum Pump Model# 1400. Ultimate vacuum: 10^{-4} torr. Oil capacity: 0.59 liter.	Fisher Scientific Phone: 1800-766-7000 http://www.fishersci.com
Glassware	Burette, mass cylinder, storage bottles.	Fisher Scientific Phone: 1800-766-7000 http://www.fishersci.com
Electronic Balance	Denver Instruments Model: SI-4002. Range: 0-4000 gm. Accuracy: 0.01 gm.	Fisher Scientific Phone: 1800-766-7000 http://www.fishersci.com
Electronic Balance	Denver Instruments. Model SI-8001. Range: 0-8000 gm. Accuracy: 0.1 gm.	Fisher Scientific Phone: 1800-766-7000 http://www.fishersci.com
Wet Test Meter	Model: 63126. Volume/rev: 3 liters. Capacity: 680 lit/h. Accuracy: 0.5% total volume.	Precision Scientific.

APPENDIX D: MS-VB® CODE FOR MS-EXCEL® DATA ACQUISITION

The Microsoft Visual-Basic® program for pressure data acquisition into MS-Excel® used in this study was developed by Darryl Bourgoyne, from the Petroleum Engineering Research and Technology Transfer Laboratory at Louisiana State University. The code to retrieve the data stored in the data set and assign it to the respective cell is published here with the permission of the developer. For the full code, contact Darryl Bourgoyne whose contact information is in Appendix C. The picture of the "Datalog" sheet in the software is shown in the Figure 20.

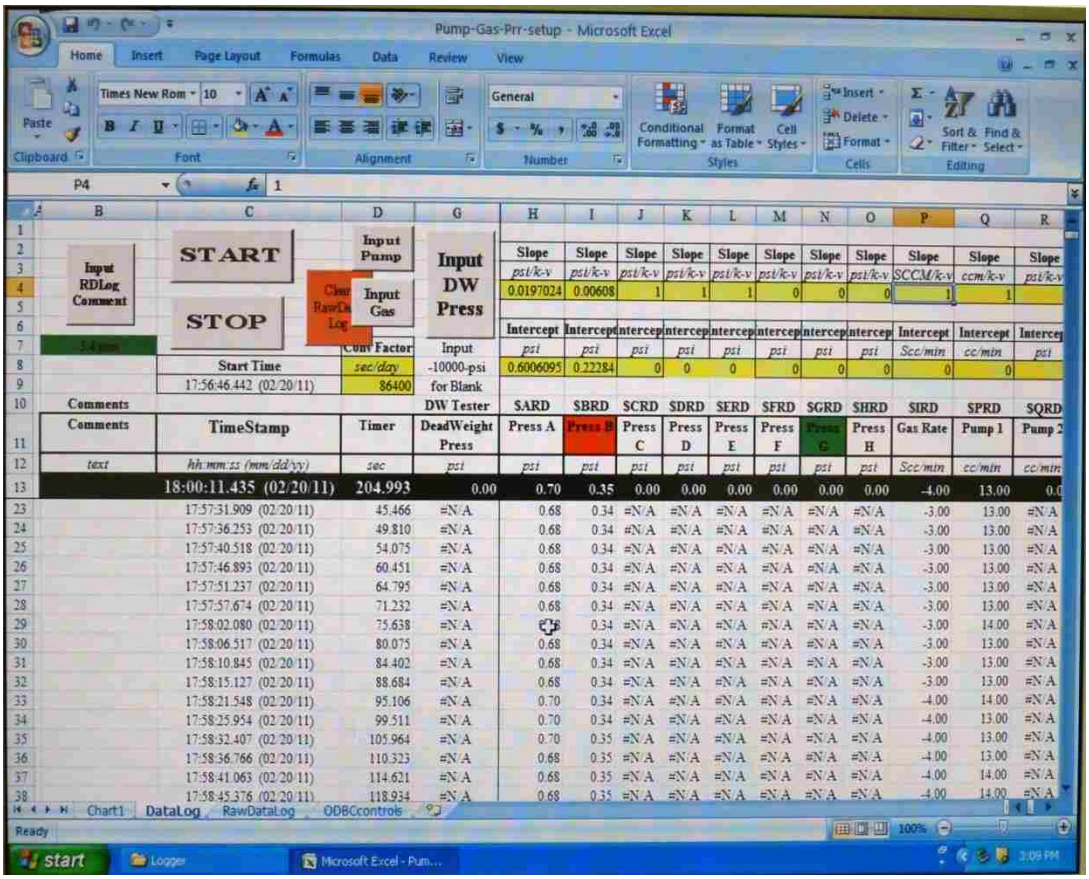

Figure 20: Datalog Sheet of MS-EXCEL® DAQ Software

The codes for the buttons in the "Datalog" and "ODBC-Control" sheets and the code to retrieve the data from the dataset into the respective cells are as follows:

BEGINNING OF CODE FOR BUTTONS IN "DATALOG" SHEET

```
Private Sub ClearRawDataLogButton_Click()

    ClearRawDataLog

End Sub
```

```
Private Sub ConfigSerialODBC_Click()

    ConfigODBC

End Sub
```

```
Private Sub KillSerialODBCbutton_Click()

    KillSerialODBC

End Sub
```

```
Private Sub LaunchSerialODBCbutton_Click()

    LaunchSerialODBC

End Sub
```

```
Private Sub Start_Click()

    StartMainSerialODBC

End Sub
```

```
Private Sub StopButton_Click()

    StopMainSerialODBC

End Sub
```

END OF CODE FOR BUTTONS IN "DATALOG" SHEET

BEGINNING OF CODE FOR BUTTONS IN "ODBC-CONTROL" SHEET

```
Private Sub ClearRawDataLogButton2_Click()

    ClearRawDataLog

End Sub
```

```
Private Sub CommentButton_Click()

    InputRawDataComment

End Sub
```

```
Private Sub InputDWpressButton_Click()

    InputDeadWeightTesterPressure

End Sub
```

```
Private Sub InputGasRateButton_Click()

    InputGasRate

End Sub
```

```
Private Sub InputPumpRateButton_Click()

    InputPumpRate

End Sub
```

```
Private Sub StartButton_Click()

    StartMainSerialODBC

End Sub
```

```
Private Sub StopButton_Click()
```

```
    StopMainSerialODBC

End Sub
```

END OF CODE FOR BUTTONS IN "ODBC-CONTROL" SHEET.

BEGINNING OF CODE FOR THE DATA ACQUISITION INTO THE CELLS

```
Public CONFIGset As Recordset

Public RXset As Recordset

Public RunFlg As Boolean

Public ODBCcontrolsSheet$

Public ODBCdatabasePath$

Public ODBCdatabaseName$

Public DeadWeightTesterValue!

Public RawDataCommentText$

Public GasRateValue!

Public PumpRateValue!
```

```
Sub GetODBCinfo()

        ODBCcontrolsSheet$ = "ODBCcontrols"

        ODBCdatabasePath$= Trim(Worksheets(ODBCcontrolsSheet$).Range("DatabasePath").Cells(1, 1))

         If Right(DatabasePath$, 1) <> "\" Then DatabasePath$ = DatabasePath$ + "\"

        ODBCdatabaseName$ = Trim(Worksheets(ODBCcontrolsSheet$).Range("DatabaseName").Cells(1, 1))

End Sub
```

```
Sub ClearRawDataLog()

        Worksheets("RawDataLog").Range("RowNumMain") = 0

        Worksheets("RawDataLog").Range("A10:AZ60000").ClearContents

End Sub
```

```
Sub InputRawDataComment()

        RawDataCommentText$ = InputBox("Input RawDataLog Comment", "RawDataLog Comment",
        RawDataCommentText$)

End Sub
```

```
Sub InputGasRate()
```

```
    GasRateValue! = InputBox("Input Gas Rate", "Gas Flowrate Data", GasRateValue!)
End Sub
```

```
Sub InputPumpRate()
    PumpRateValue! = InputBox("Input Pump Rate", "Pump Rate Data", PumpRateValue!)
End Sub
```

```
Sub StartMainSerialODBC()
    GetODBCinfo
    TableMapSheet$ = ODBCcontrolsSheet$
    RunFlg = True
    Worksheets(TableMapSheet$).Range("RunFlg") = RunFlg
    MainSerialODBC
End Sub
```

```
Sub StopMainSerialODBC()
    GetODBCinfo
    TableMapSheet$ = ODBCcontrolsSheet$
    RunFlg = False
    Worksheets(TableMapSheet$).Range("RunFlg") = RunFlg
End Sub
```

```
Sub MainSerialODBC()

  GetODBCinfo

  TableMapSheet$ = ODBCcontrolsSheet$
  DatabasePath$ = ODBCdatabasePath$
  DatabaseName$ = ODBCdatabaseName$

  LaunchSerialODBC

  Worksheets(TableMapSheet$).Range("ExcelComMessage") = "Initializing MainExcelCom()"
  Worksheets(TableMapSheet$).Range("ExcelComErrors") = "NO ERRORS"
```

```
Set SerialODBCDataBase = OpenDatabase(DatabasePath$ + DatabaseName$)
Set RXset = SerialODBCDataBase.OpenRecordset("RX")
Set CONFIGset = SerialODBCDataBase.OpenRecordset("Config")

Verror! = -10000
DelayTime1 = Worksheets(TableMapSheet$).Range("DelayTime1")
DelayTime2 = Worksheets(TableMapSheet$).Range("DelayTime2")
DelayTime3 = Worksheets(TableMapSheet$).Range("DelayTime3")

Worksheets(TableMapSheet$).Range("ExcelComMessage") = "Executing MainExcelCom's Primary DO-LOOP"

RowNumMain& = Worksheets("RawDataLog").Range("RowNumMain")

DeadWeightTesterValue = Verror!
GasRateValue! = Verror!
PumpRateValue! = Verror!
RawDataCommentText$ = ""

TimedDelay (DelayTime1)

Do

   TimedDelay (DelayTime2)     'Wait for Command to be sent and Module to reply

   OldTimeStamp$ = NewTimeStamp$
   NewTimeStamp$ = RXset.Fields("TimeStamp")   'Poll ODBC database for RX timestamp

   If Val (NewTimeStamp$) > Verror! And OldTimeStamp$ <> NewTimeStamp$ And RunFlg = True Then

        RowNumMain& = RowNumMain& + 1
        Worksheets("RawDataLog").Range("RowNumMain") = RowNumMain&
```

```
        If Len(RawDataCommentText$) > 0 Then
            Worksheets("RawDataLog").Range("A10").Cells(RowNumMain&, 1) = RawDataCommentText$
            RawDataCommentText$ = ""
          Else
            Worksheets("RawDataLog").Range("A10").Cells(RowNumMain&, 1).ClearContents
        End If

        If DeadWeightTesterValue > Verror! Then
            Worksheets("RawDataLog").Range("B10").Cells(RowNumMain&, 1) = DeadWeightTesterValue
          Else
            Worksheets("RawDataLog").Range("B10").Cells(RowNumMain&, 1).ClearContents
        End If

        If GasRateValue! > Verror! Then
            Worksheets("RawDataLog").Range("C10").Cells(RowNumMain&, 1) = GasRateValue!
          Else
            Worksheets("RawDataLog").Range("C10").Cells(RowNumMain&, 1).ClearContents
        End If

        If PumpRateValue! > Verror! Then
            Worksheets("RawDataLog").Range("D10").Cells(RowNumMain&, 1) = PumpRateValue!
          Else
            Worksheets("RawDataLog").Range("D10").Cells(RowNumMain&, 1).ClearContents
        End If


'&&&&&&&&&&&&&&&&&&&&&&&&&&&&&&&&&&&&&&&&&&&&&&&&&&&&&&&&&&&&&&&&&&&&&&&&&&&&&&&&&&&&&&&&&&&&&&&&&&&&&&&&
        'Logging COM Polled Data

'&&&&&&&&&&&&&&&&&&&&&&&&&&&&&&&&&&&&&&&&&&&&&&&&&&&&&&&&&&&&&&&&&&&&&&&&&&&&&&&&&&&&&&&&&&&&&&&&&&&&&&&&
```

```
        'D$ = RXset.Fields("TimeStamp")                    'Poll ODBC database for RX timestamp
        If Left(NewTimeStamp$, 1) = "'" Then
            D$ = Right(NewTimeStamp$, Len(NewTimeStamp$) - 1)  'Clean-up Timestamp
          Else
            D$ = NewTimeStamp$
        End If

        DataCol% = 1
        Worksheets("RawDataLog").Range("E10").Cells(RowNumMain&, DataCol%) = D$     'Write Timestamp to RawDataLog Sheet

        V! = Val(RXset.Fields("$ARD"))
        DataCol% = DataCol% + 1
        If V! > Verror! Then
            Worksheets("RawDataLog").Range("E10").Cells(RowNumMain&, DataCol%) = V!
          Else
            Worksheets("RawDataLog").Range("E10").Cells(RowNumMain&, DataCol%).ClearContents
        End If
        DataCol% = DataCol% + 1
        Worksheets("RawDataLog").Range("E10").Cells(RowNumMain&, DataCol%) = RXset.Fields("$ARDmessage")

        V! = Val(RXset.Fields("$BRD"))
        DataCol% = DataCol% + 1
        If V! > Verror! Then
            Worksheets("RawDataLog").Range("E10").Cells(RowNumMain&, DataCol%) = V!
          Else
            Worksheets("RawDataLog").Range("E10").Cells(RowNumMain&, DataCol%).ClearContents
        End If
        DataCol% = DataCol% + 1
        Worksheets("RawDataLog").Range("E10").Cells(RowNumMain&, DataCol%) = RXset.Fields("$BRDmessage")
```

```
        V! = Val(RXset.Fields("$CRD"))
        DataCol% = DataCol% + 1
        If V! > Verror! Then
            Worksheets("RawDataLog").Range("E10").Cells(RowNumMain&, DataCol%) = V!
          Else
            Worksheets("RawDataLog").Range("E10").Cells(RowNumMain&, DataCol%).ClearContents
        End If
        DataCol% = DataCol% + 1
        Worksheets("RawDataLog").Range("E10").Cells(RowNumMain&, DataCol%) =
RXset.Fields("$CRDmessage")

        V! = Val(RXset.Fields("$DRD"))
        DataCol% = DataCol% + 1
        If V! > Verror! Then
            Worksheets("RawDataLog").Range("E10").Cells(RowNumMain&, DataCol%) = V!
          Else
            Worksheets("RawDataLog").Range("E10").Cells(RowNumMain&, DataCol%).ClearContents
        End If
        DataCol% = DataCol% + 1
        Worksheets("RawDataLog").Range("E10").Cells(RowNumMain&, DataCol%) =
RXset.Fields("$DRDmessage")

        V! = Val(RXset.Fields("$ERD"))
        DataCol% = DataCol% + 1
        If V! > Verror! Then
            Worksheets("RawDataLog").Range("E10").Cells(RowNumMain&, DataCol%) = V!
          Else
            Worksheets("RawDataLog").Range("E10").Cells(RowNumMain&, DataCol%).ClearContents
        End If
        DataCol% = DataCol% + 1
        Worksheets("RawDataLog").Range("E10").Cells(RowNumMain&, DataCol%) =
RXset.Fields("$ERDmessage")
```

```
        V! = Val(RXset.Fields("$FRD"))
        DataCol% = DataCol% + 1
        If V! > Verror! Then
            Worksheets("RawDataLog").Range("E10").Cells(RowNumMain&, DataCol%) = V!
          Else
            Worksheets("RawDataLog").Range("E10").Cells(RowNumMain&, DataCol%).ClearContents
        End If
        DataCol% = DataCol% + 1
        Worksheets("RawDataLog").Range("E10").Cells(RowNumMain&, DataCol%) =
RXset.Fields("$FRDmessage")

        V! = Val(RXset.Fields("$GRD"))
        DataCol% = DataCol% + 1
        If V! > Verror! Then
            Worksheets("RawDataLog").Range("E10").Cells(RowNumMain&, DataCol%) = V!
          Else
            Worksheets("RawDataLog").Range("E10").Cells(RowNumMain&, DataCol%).ClearContents
        End If
        DataCol% = DataCol% + 1
        Worksheets("RawDataLog").Range("E10").Cells(RowNumMain&, DataCol%) =
RXset.Fields("$GRDmessage")

        V! = Val(RXset.Fields("$HRD"))
        DataCol% = DataCol% + 1
        If V! > Verror! Then
            Worksheets("RawDataLog").Range("E10").Cells(RowNumMain&, DataCol%) = V!
          Else
            Worksheets("RawDataLog").Range("E10").Cells(RowNumMain&, DataCol%).ClearContents
        End If
        DataCol% = DataCol% + 1
        Worksheets("RawDataLog").Range("E10").Cells(RowNumMain&, DataCol%) =
RXset.Fields("$HRDmessage")
```

```
        V! = Val(RXset.Fields("$IRD"))
        DataCol% = DataCol% + 1
        If V! > Verror! Then
            Worksheets("RawDataLog").Range("E10").Cells(RowNumMain&, DataCol%) = V!
          Else
            Worksheets("RawDataLog").Range("E10").Cells(RowNumMain&, DataCol%).ClearContents
        End If
        DataCol% = DataCol% + 1
        Worksheets("RawDataLog").Range("E10").Cells(RowNumMain&, DataCol%) =
RXset.Fields("$IRDmessage")

        V! = Val(RXset.Fields("$PRD"))
        DataCol% = DataCol% + 1
        If V! > Verror! Then
            Worksheets("RawDataLog").Range("E10").Cells(RowNumMain&, DataCol%) = V!
          Else
            Worksheets("RawDataLog").Range("E10").Cells(RowNumMain&, DataCol%).ClearContents
        End If
        DataCol% = DataCol% + 1
        Worksheets("RawDataLog").Range("E10").Cells(RowNumMain&, DataCol%) =
RXset.Fields("$PRDmessage")

        V! = Val(RXset.Fields("$QRD"))
        DataCol% = DataCol% + 1
        If V! > Verror! Then
            Worksheets("RawDataLog").Range("E10").Cells(RowNumMain&, DataCol%) = V!
          Else
            Worksheets("RawDataLog").Range("E10").Cells(RowNumMain&, DataCol%).ClearContents
        End If
        DataCol% = DataCol% + 1
       Worksheets("RawDataLog").Range("E10").Cells(RowNumMain&, DataCol%) =
       RXset.Fields("$QRDmessage")
```

```
'&&&&&&&&&&&&&&&&&&&&&&&&&&&&&&&&&&&&&&&&&&&&&&&&&&&&&&&&&&&&
&&&&&&&&&&&&&&&&&&&&&&&&&&&&&&&&&&&&

            '<END> Logging COM Polled Data

'^^^^^^^^^^^^^^^^^^^^^^^^^^^^^^^^^^^^^^^^^^^^^^^^^^^^^^^^^^^^^^^^^^^^^^^^^^^^^^^^^^^^^^^^^^^^^^^^^^

      End If

   RunFlg = Worksheets(TableMapSheet$).Range("RunFlg")

   TimedDelay (DelayTime3)

   Loop While RunFlg = True

   Worksheets(TableMapSheet$).Range("ExcelComMessage") = "Exited MainExcelCom's Primary DO-LOOP"

   CONFIGset.Edit
   Worksheets(TableMapSheet$).Range("ODBC_Config_RunFlg").Cells(1, 1) = 0
   CONFIGset.Fields("RunFlg") = Worksheets(TableMapSheet$).Range("ODBC_Config_RunFlg").Cells(1, 1)
   CONFIGset.Update
   Worksheets(TableMapSheet$).Range("ODBC_Config_RunFlg").Cells(1, 2) = CONFIGset.Fields("RunFlg")

   RXset.Close
   CONFIGset.Close
   SerialODBCDataBase.Close

   Worksheets(TableMapSheet$).Range("ExcelComMessage") = "Ended MainExcelCom()"

End Sub
```

```
Sub TimedDelay(T)

   'T is in ms
```

```
    Static StartTime As Single

    StartTime = Timer

    Do

        DoEvents
        Calculate

    Loop While Abs(Timer - StartTime) < T / 1000 And RunFlg = True

End Sub
```

```
Sub ConfigODBC()

    GetODBCinfo

    TableMapSheet$ = ODBCcontrolsSheet$
    DatabasePath$ = ODBCdatabasePath$
    DatabaseName$ = ODBCdatabaseName$

    Set SerialODBCDataBase = OpenDatabase(DatabasePath$ + DatabaseName$)
    Set CONFIGset = SerialODBCDataBase.OpenRecordset("Config")

    Worksheets(TableMapSheet$).Range("ODBC_Config_RunFlg").Cells(1, 1) = -1

    CONFIGset.Edit

    CONFIGset.Fields("RunFlg") = Worksheets(TableMapSheet$).Range("ODBC_Config_RunFlg").Cells(1, 1)
    CONFIGset.Fields("NumChannels") =
Worksheets(TableMapSheet$).Range("ODBC_Config_NumChannels").Cells(1, 1)
    CONFIGset.Fields("OpenComParam") =
Worksheets(TableMapSheet$).Range("ODBC_Config_OpenComParam").Cells(1, 1)
```

```
    CONFIGset.Fields("ResponseWait")                                    =
Worksheets(TableMapSheet$).Range("ODBC_Config_ResponseWait").Cells(1, 1)

    CONFIGset.Fields("ResponseWaitLong")                                =
Worksheets(TableMapSheet$).Range("ODBC_Config_ResponseWaitLong").Cells(1, 1)

    CONFIGset.Fields("ResponseTimeOut")                                 =
Worksheets(TableMapSheet$).Range("ODBC_Config_ResponseTimeOut").Cells(1, 1)


    CONFIGset.Update


    Worksheets(TableMapSheet$).Range("ODBC_Config_RunFlg").Cells(1, 2) = CONFIGset.Fields("RunFlg")

    Worksheets(TableMapSheet$).Range("ODBC_Config_NumChannels").Cells(1,          2)        =
CONFIGset.Fields("NumChannels")

    Worksheets(TableMapSheet$).Range("ODBC_Config_OpenComParam").Cells(1,          2)       =
CONFIGset.Fields("OpenComParam")

    Worksheets(TableMapSheet$).Range("ODBC_Config_ResponseWait").Cells(1,          2)       =
CONFIGset.Fields("ResponseWait")

    Worksheets(TableMapSheet$).Range("ODBC_Config_ResponseWaitLong").Cells(1,          2)   =
CONFIGset.Fields("ResponseWaitLong")

    Worksheets(TableMapSheet$).Range("ODBC_Config_ResponseTimeOut").Cells(1,          2)    =
CONFIGset.Fields("ResponseTimeOut")


    CONFIGset.Close

    SerialODBCDataBase.Close


End Sub
```

```
Sub LaunchSerialODBC()


    GetODBCinfo


    TableMapSheet$ = ODBCcontrolsSheet$

    DatabasePath$ = ODBCdatabasePath$

    DatabaseName$ = ODBCdatabaseName$


    ConfigODBC
```

```
    D$ = CurDir

    ExeName$ = Trim(Worksheets(TableMapSheet$).Range("SerialODBC_Exe").Cells(1, 1))

    ChDrive Left(DatabasePath$, 1)
    ChDir DatabasePath$

    R = Shell(ExeName$ + " " + DatabaseName$, vbNormalNoFocus)

    ChDrive Left(D$, 1)
    ChDir D$

End Sub
```

```
Sub KillSerialODBC()

    GetODBCinfo

    TableMapSheet$ = ODBCcontrolsSheet$
    DatabasePath$ = ODBCdatabasePath$
    DatabaseName$ = ODBCdatabaseName$

    Set SerialODBCDataBase = OpenDatabase(DatabasePath$ + DatabaseName$)
    Set CONFIGset = SerialODBCDataBase.OpenRecordset("Config")

    Worksheets(TableMapSheet$).Range("ODBC_Config_RunFlg").Cells(1, 1) = 0

    CONFIGset.Edit

    CONFIGset.Fields("RunFlg") = Worksheets(TableMapSheet$).Range("ODBC_Config_RunFlg").Cells(1, 1)

    CONFIGset.Update
```

```
Worksheets(TableMapSheet$).Range("ODBC_Config_RunFlg").Cells(1, 2) = CONFIGset.Fields("RunFlg")


CONFIGset.Close

SerialODBCDataBase.Close


End Sub
```

END OF CODE FOR THE DATA ACQUISITION INTO THE CELLS

VITA

Shrinidhi Shetty is a native of Mangalore, Karnataka, India. He was born in May, 1983 in Davangere, Karnataka. He did his schooling from Kendriya Vidyalaya Dharwad. He earned his Bachelor of Engineering in Mechanical Engineering degree from Visvesvaraya Technological University, Belgaum, India in 2005. He will be awarded the degree of Master of Science in Petroleum Engineering during the spring commencement of 2011. His technical interests are multiphase fluid flows and enhanced oil recovery.